Transverse momentum resummation in Drell-Yan pair production: a progress report

Luca Rottoli

LHC EW WG general meeting, 10 July, CERN

Transverse observables in Drell-Yan pair production

Neutral and charged current Drell-Yan production is central to the precision programme at hadron colliders thanks to its **large cross section** and **clean experimental signature**

Kinematic distributions which involve the production of a lepton pair in association with QCD radiation play a special role, as they are sensitive to accompanying hadronic activity **only through kinematic recoil**

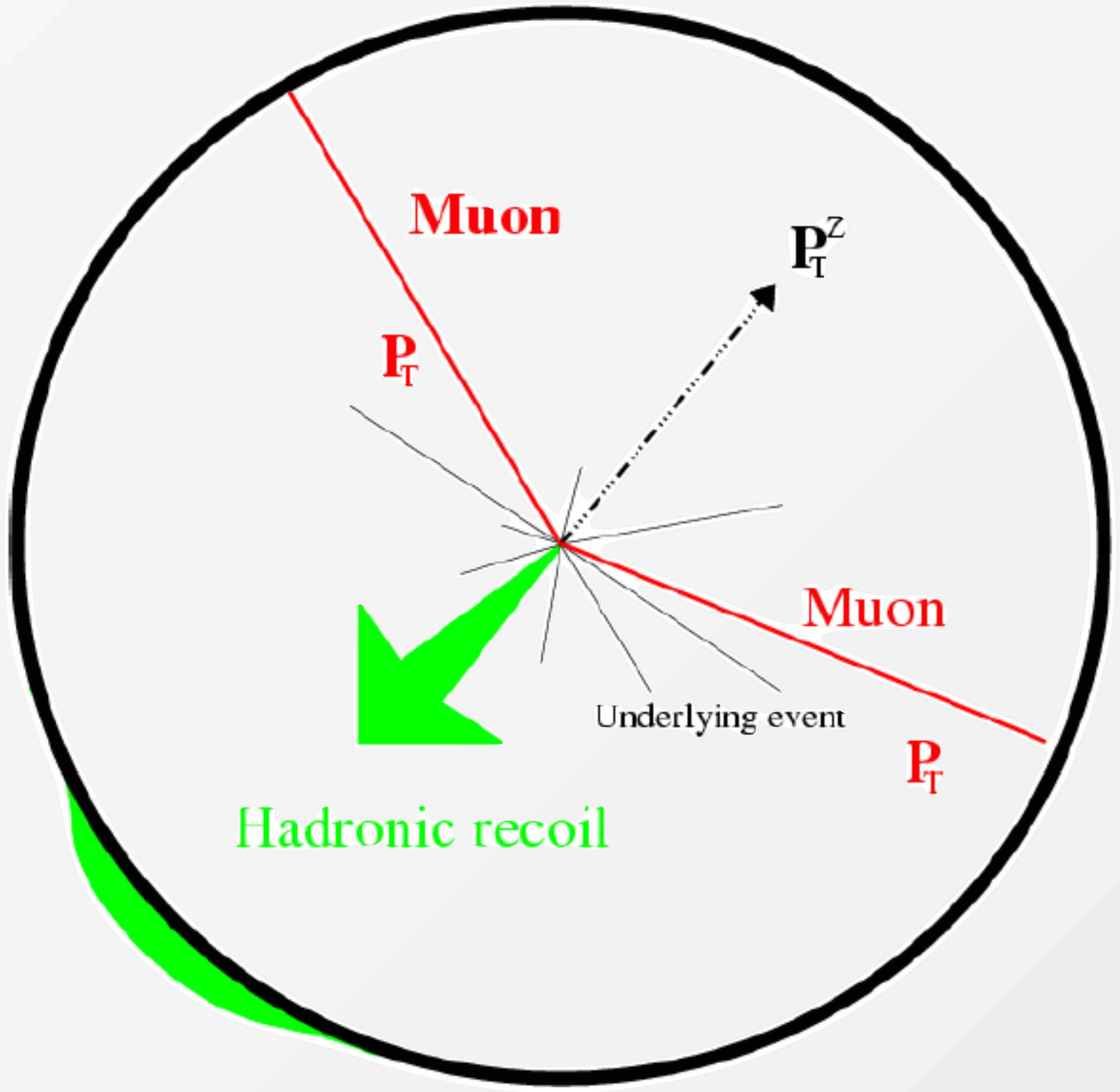

→ Measurement of transverse and angular observables often lead to small experimental uncertainties

W/*Z* spectra at small transverse momentum: fixed order

Great experimental precision of the Z p_t spectrum (sub-% level) challenges current theory predictions

State of the art for fixed order p_t spectrum is NNLO: Z/W recoiling against at least one hard radiation

[Gehrmann-De Ridder, Gehrmann, Glover, Huss, Morgan, Walker 2015-2017]
[Boughezal, Campbell, Ellis, Focke, Giele, Liu, Petriello 2015]

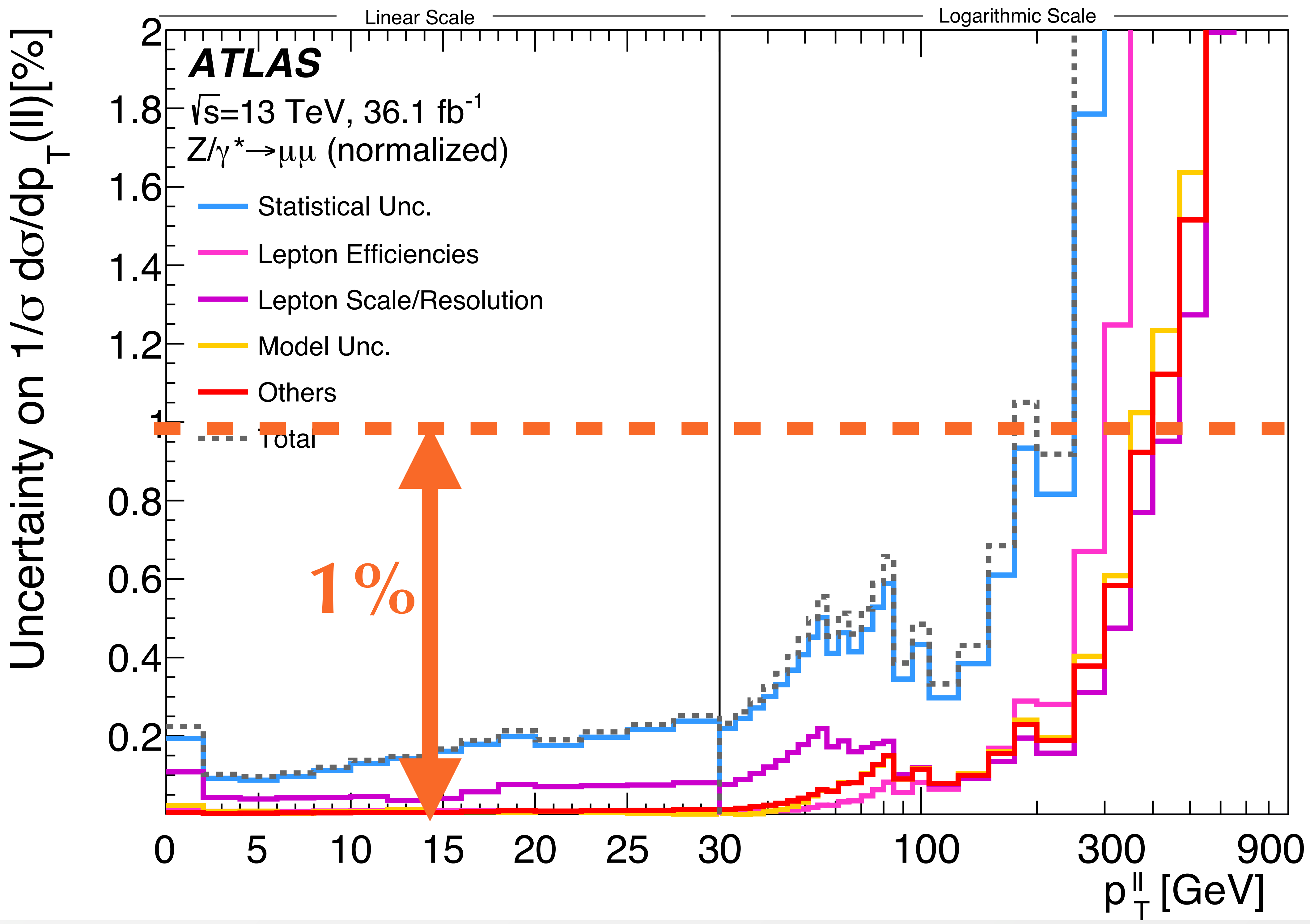

[ATLAS 2019]

Fixed-order perturbative description breaks in the $p_T \to 0$ limit, due to the appearance of large logarithms of $p_T/m_{\ell\ell}$, which must be resummed lest they spoil the perturbative convergence

W/*Z* spectra at small transverse momentum: resummation

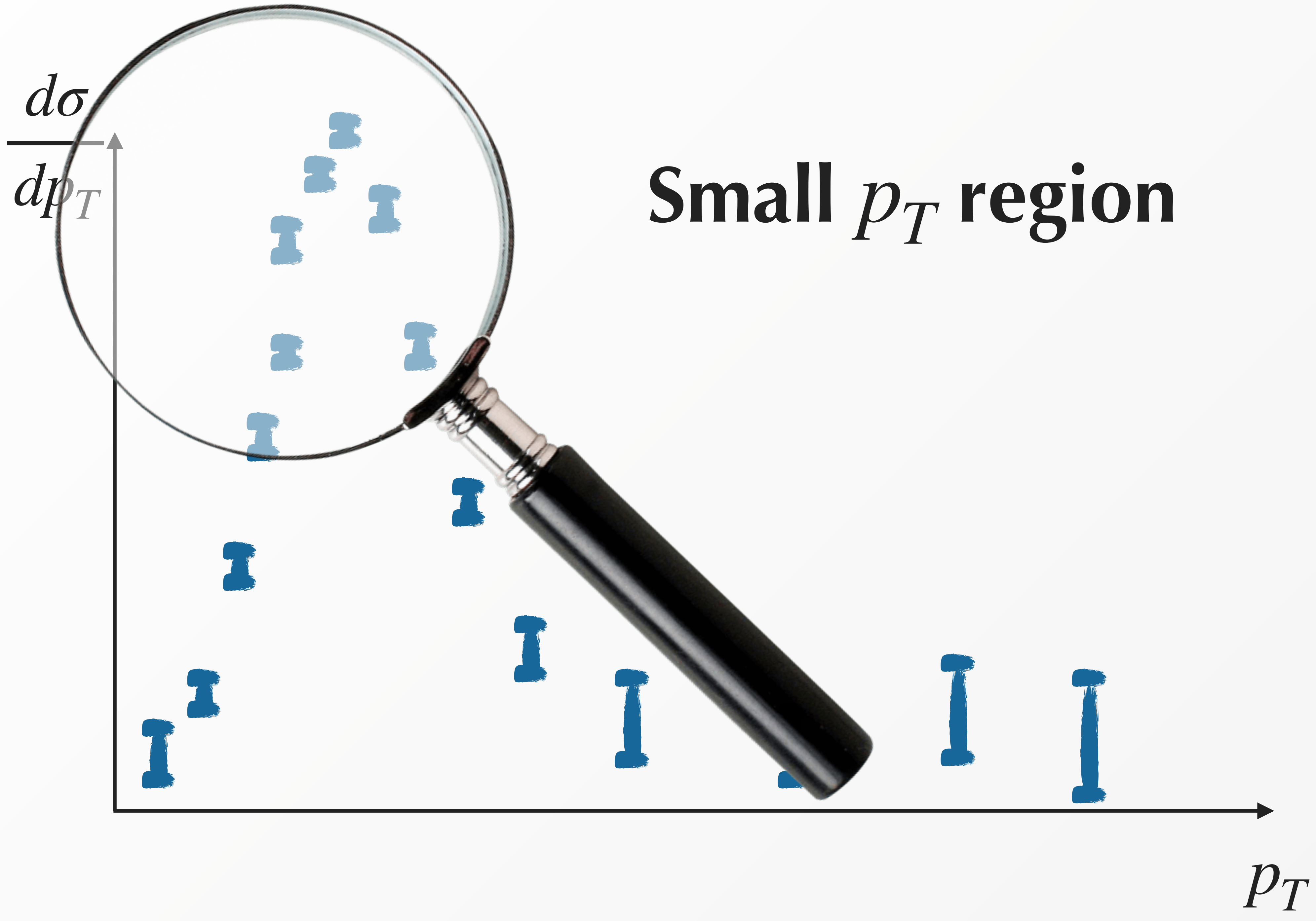

Small p_T region

Double logarithms **leftovers** of the real-virtual cancellation of IRC divergences

$$\tilde{\sigma}_1(p_T) \sim \underbrace{\int \frac{d\theta}{\theta}\frac{dE}{E}\Theta\left(p_T - E\theta\right)}_{} - \underbrace{\int \frac{d\theta}{\theta}\frac{dE}{E}}_{}$$

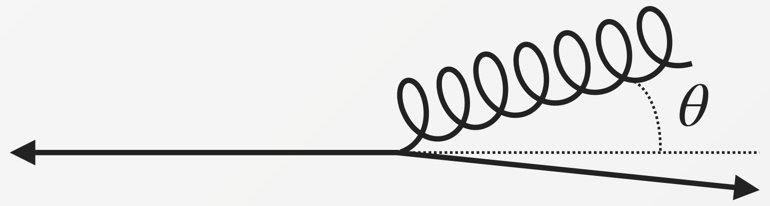

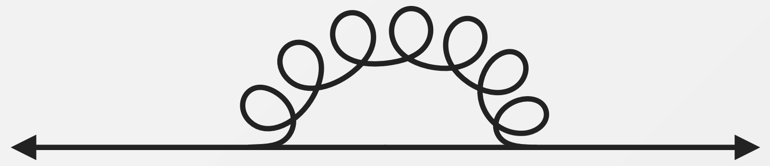

$$\sim -\int \frac{dE}{E}\frac{d\theta}{\theta}\Theta(E\theta - p_T) \sim -\frac{1}{2}\ln^2\frac{p_T}{m_{\ell\ell}}$$ **Sudakov logarithms**

Origin of the logs is simple. Resum them to all orders by **reorganizing** the series

$$\ln\tilde{\sigma}(p_T) = \sum_n \left(\mathcal{O}(\alpha_s^n L^{n+1}) + \mathcal{O}(\alpha_s^n L^n) + \mathcal{O}(\alpha_s^n L^{n-1}) + \dots\right)$$

LL **NLL** **NNLL**

$$L = \ln(p_T/m_{\ell\ell})$$

Resummation of the transverse momentum spectrum

Resummation of transverse momentum is delicate because p_T is a **vectorial quantity**

Two concurring mechanisms leading to a system with small p_T

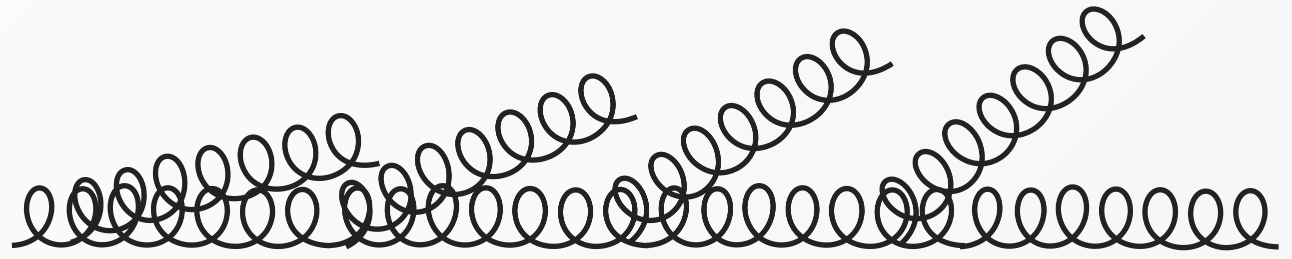

$$p_\perp^2 \sim k_{t,i}^2 \ll m_H^2$$

cross section naturally suppressed as there is no phase space left for gluon emission (Sudakov limit)

Exponential suppression

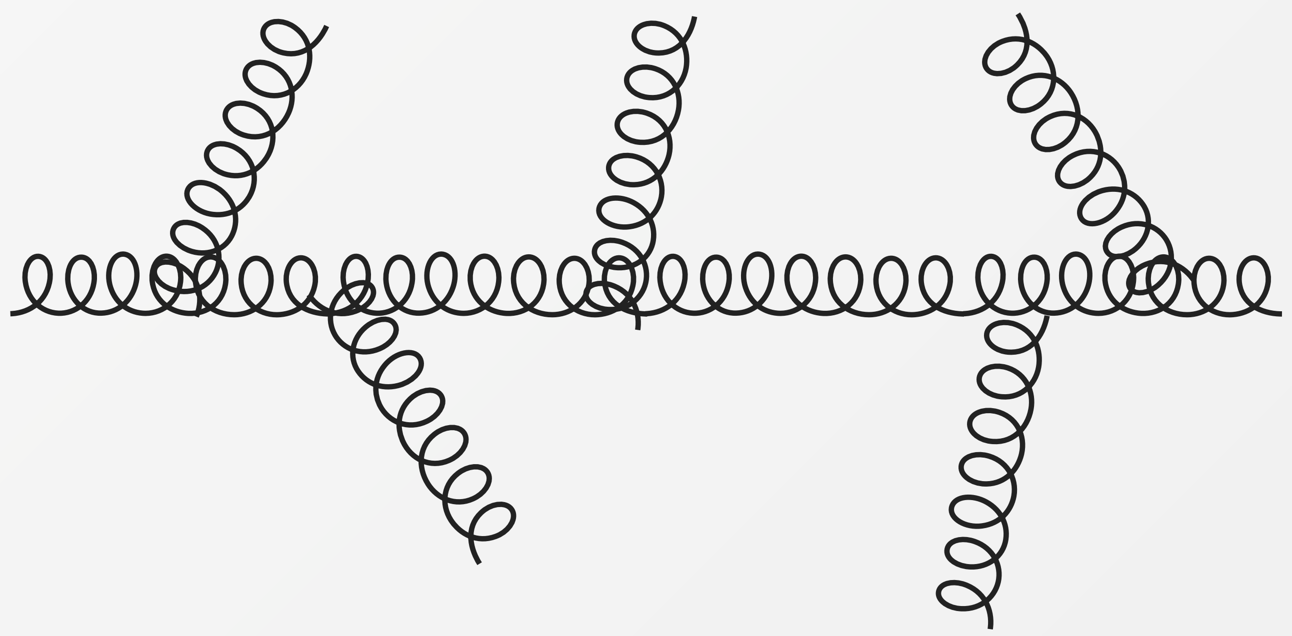

$$\sum_{i=1}^{n} \vec{k}_{t,i} \simeq 0$$

Large kinematic cancellations

$p_T \sim 0$ far from the Sudakov limit

Power suppression

Resummation of the transverse momentum spectrum

Resummation of transverse momentum is delicate because p_T is a **vectorial quantity**

Two concurring mechanisms leading to a system with small p_T

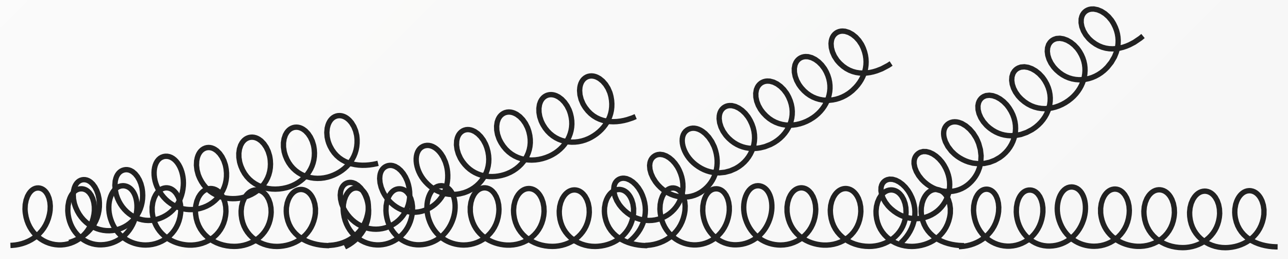

$$p_\perp^2 \sim k_{t,i}^2 \ll m_H^2$$

cross section naturally suppressed as there is no phase space left for gluon emission (Sudakov limit)

Exponential suppression

Dominant at small p_T

$$\sum_{i=1}^{n} \vec{k}_{t,i} \simeq 0$$

Large kinematic cancellations

$p_T \sim 0$ far from the Sudakov limit

Power suppression

Impact-parameter space approach

The two competing effects are usually handled in **impact parameter** (b) space, where the phase-space constraints factorise

$$\delta^{(2)}\left(\vec{p}_T - \sum_{i=1}^{n} \vec{k}_{t,i}\right) = \int d^2b \frac{1}{4\pi^2} e^{i\vec{b}\cdot\vec{p}_T} \prod_{i=1}^{n} e^{-i\vec{b}\cdot\vec{k}_{t,i}}$$

two-dimensional momentum conservation

[Parisi, Petronzio 1979][Collins, Soper, Sterman 1985]

Exponentiation in conjugate space; **inverse transform** to move back to direct space

NLL formula with scale-independent PDFs

$$\sigma = \sigma_0 \int d^2\vec{p}_T \int \frac{d^2\vec{b}}{4\pi^2} e^{-i\vec{b}\cdot\vec{p}_T} \sum_{n=0}^{\infty} \frac{1}{n!} \prod_{i=1}^{n} \int [dk_i] |M(k_i)|^2 \left(e^{i\vec{b}\cdot\vec{k}_{t,i}} - 1\right)$$

$$= \sigma_0 \int d^2\vec{p}_T \int \frac{d^2\vec{b}}{4\pi^2} e^{-i\vec{b}\cdot\vec{p}_T} e^{-R_{\mathrm{NLL}}(L)}$$

virtual corrections

$$R_{\mathrm{NLL}}(L) = -L g_1(\alpha_s L) - g_2(\alpha_s L)$$

$$L = \ln(m_{\ell\ell} b / b_o) \qquad b_0 = 2e^{-\gamma_E}$$

Extremely successful approach; resummation for DY production performed within a variety of formalisms (**direct QCD**, **SCET**, **TMD**)

Impact-parameter space approach: direct QCD

Factorization in **direct QCD** for production of color-less system F: (Q^2, Y, q_T)

[Catani, de Florian, Grazzini, 2001]

$$\frac{d\sigma^{(sing)}}{dQ^2 dY dp_T d\Omega} = \frac{1}{S}\sum_c \frac{d\sigma^{(0)}_{c\bar{c},F}}{d\Omega}\int_0^\infty db\frac{b}{2}J_0(bp_T)S_c(Q,b)\sum_{a_1,a_2}\int_{x_1}^1\frac{dz_1}{z_1}\int_{x_2}^1\frac{dz_2}{z_2}[H^F C_1 C_2]_{c\bar{c};a_1a_2} f_{a_1/h_1}(x_1, b_0^2/b^2) f_{a_2/h_2}(x_2, b_0^2/b^2)$$

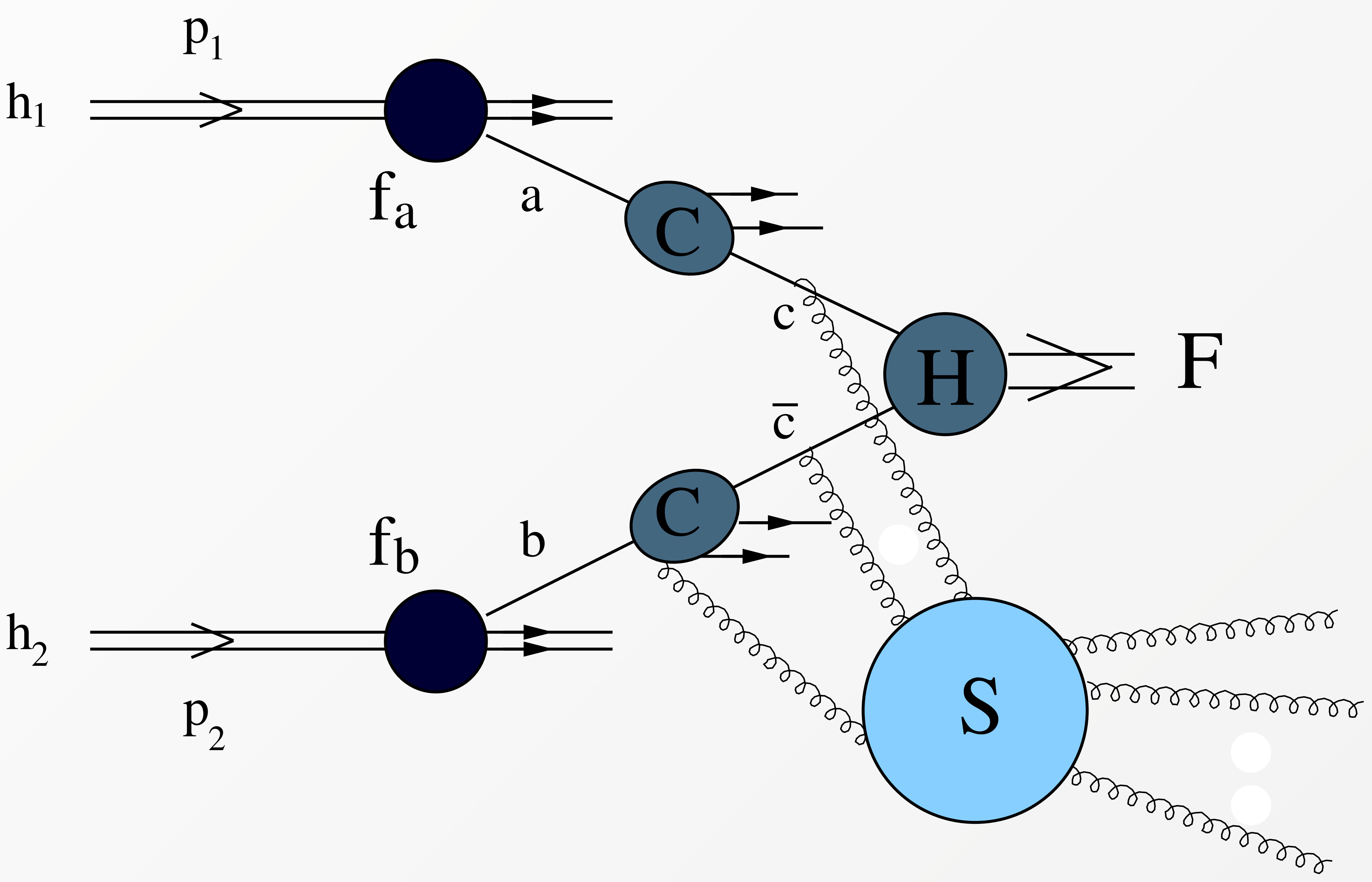

Impact-parameter space approach: direct QCD

Factorization in **direct QCD** for production of color-less system F: (Q^2, Y, q_T)

[Catani, de Florian, Grazzini, 2001]

$$\frac{d\sigma^{(sing)}}{dQ^2 dY dp_T d\Omega} = \frac{1}{S}\sum_c \frac{d\sigma^{(0)}_{c\bar{c},F}}{d\Omega}\int_0^\infty db\frac{b}{2}J_0(bp_T)S_c(Q,b)\sum_{a_1,a_2}\int_{x_1}^1\frac{dz_1}{z_1}\int_{x_2}^1\frac{dz_2}{z_2}[H^F C_1 C_2]_{c\bar{c};a_1a_2} f_{a_1/h_1}(x_1, b_0^2/b^2) f_{a_2/h_2}(x_2, b_0^2/b^2)$$

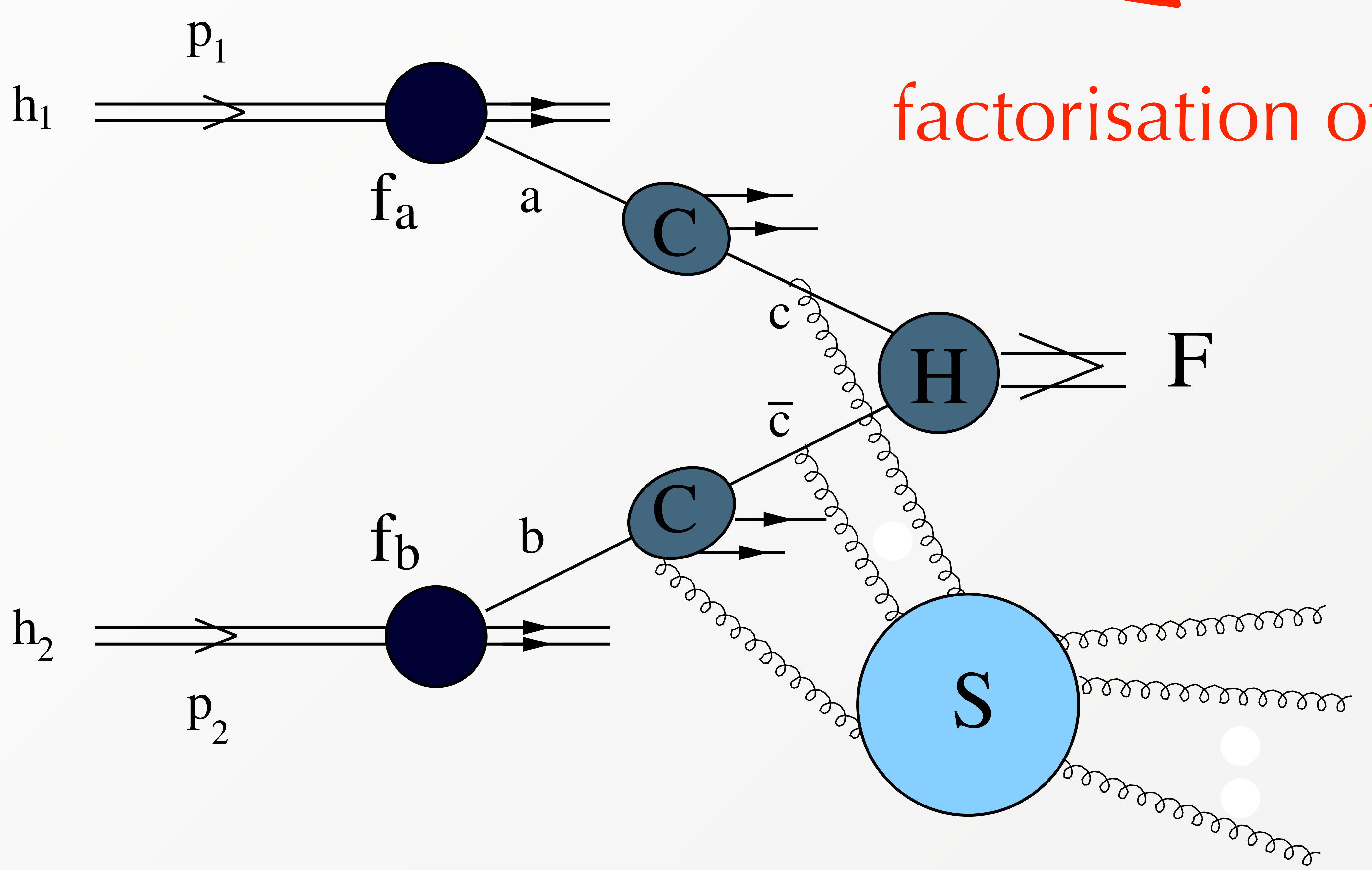

factorisation of the constraint $\delta^2\left(\mathbf{p}_T - \sum_i \mathbf{k}_{T,i}\right)$ in ***b* space**

Impact-parameter space approach: direct QCD

Factorization in **direct QCD** for production of color-less system F: (Q^2, Y, q_T)

[Catani, de Florian, Grazzini, 2001]

$$\frac{d\sigma^{(sing)}}{dQ^2 dY dp_T d\Omega} = \frac{1}{S}\sum_c \frac{d\sigma^{(0)}_{c\bar{c},F}}{d\Omega}\int_0^\infty db\frac{b}{2}J_0(bp_T)S_c(Q,b)\sum_{a_1,a_2}\int_{x_1}^1\frac{dz_1}{z_1}\int_{x_2}^1\frac{dz_2}{z_2}[H^F C_1 C_2]_{c\bar{c};a_1a_2} f_{a_1/h_1}(x_1, b_0^2/b^2) f_{a_2/h_2}(x_2, b_0^2/b^2)$$

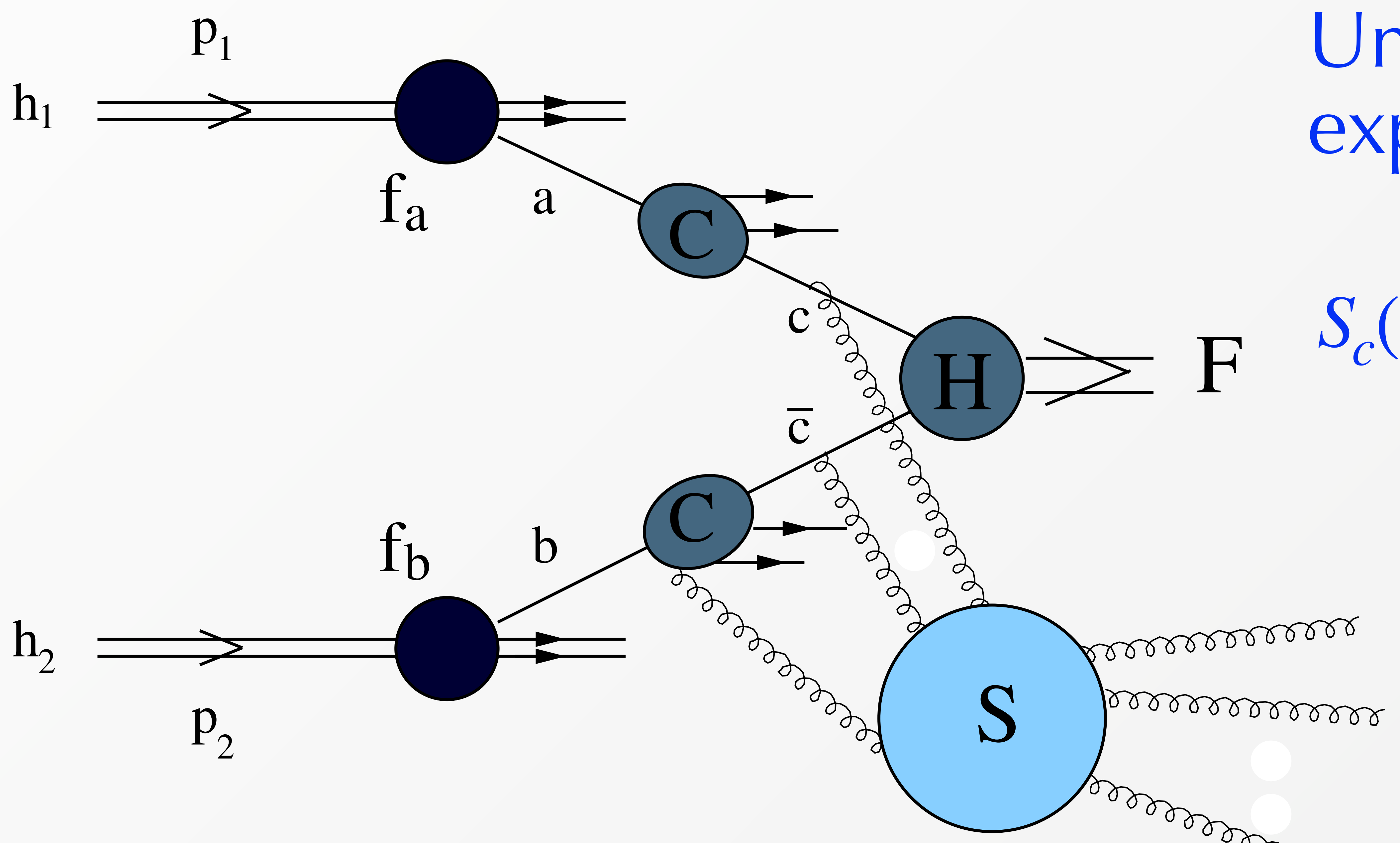

Universal **Sudakov Form Factor**:
exponentiation of soft-collinear emissions

$$S_c(Q,b) = \exp\left[-\int_{b_0^2/b^2}^{Q^2} dq^2 A_c\left(\alpha_S(q^2)\right)\ln\frac{Q^2}{q^2} + B_c\left(\alpha_S(q^2)\right)\right]$$

A_c, B_c admits a perturbative expansion in α_S

Impact-parameter space approach: direct QCD

Factorization in **direct QCD** for production of color-less system F: (Q^2, Y, q_T)

[Catani, de Florian, Grazzini, 2001]

$$\frac{d\sigma^{(sing)}}{dQ^2 dY dp_T d\Omega} = \frac{1}{S}\sum_c \frac{d\sigma^{(0)}_{c\bar{c},F}}{d\Omega}\int_0^\infty db \frac{b}{2} J_0(bp_T) S_c(Q,b) \sum_{a_1,a_2}\int_{x_1}^1 \frac{dz_1}{z_1}\int_{x_2}^1 \frac{dz_2}{z_2} [H^F C_1 C_2]_{c\bar{c};a_1a_2} f_{a_1/h_1}(x_1, b_0^2/b^2) f_{a_2/h_2}(x_2, b_0^2/b^2)$$

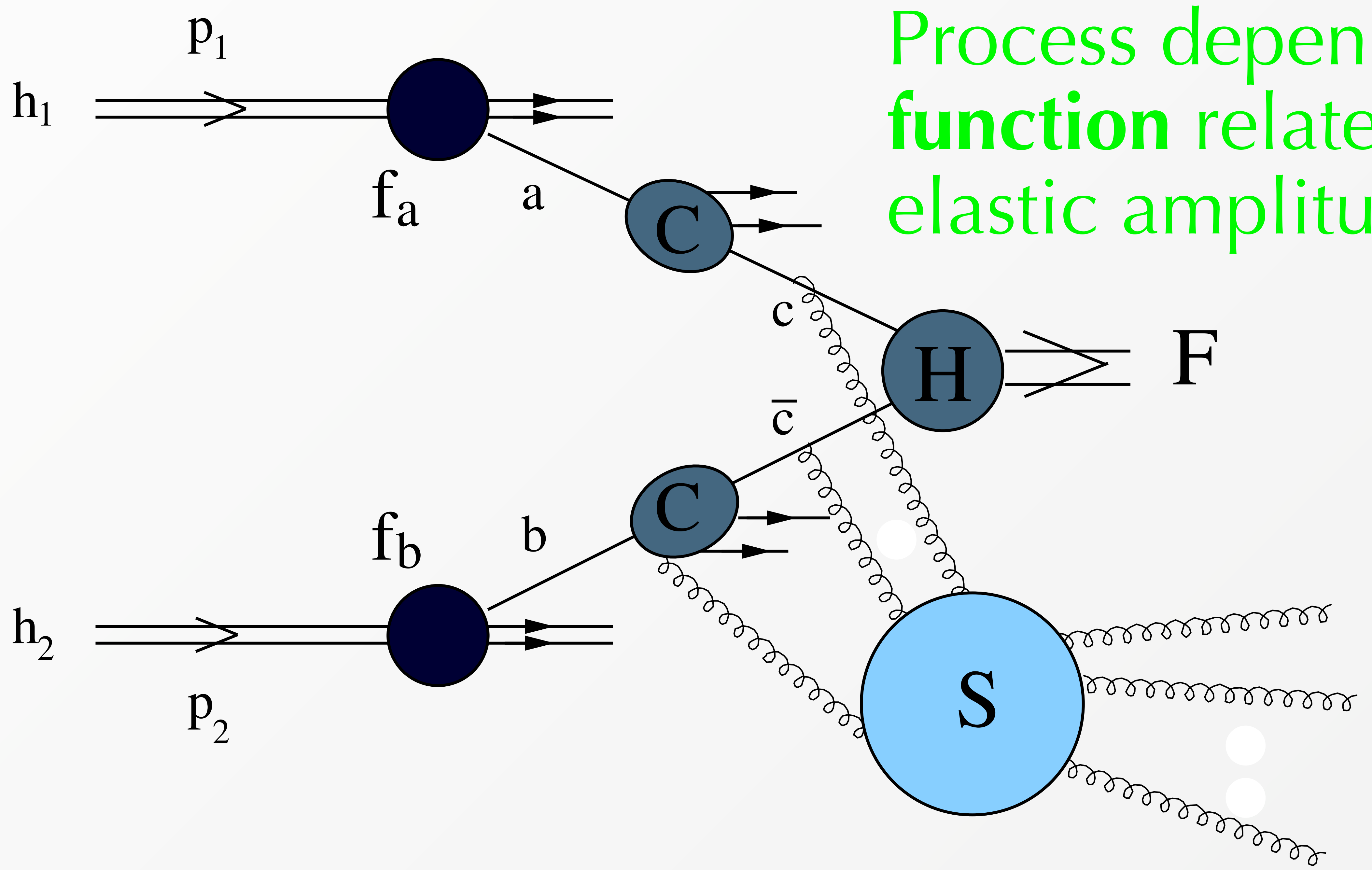

Process dependent **Hard-Virtual function** related to the all-order elastic amplitude

Universal **collinear or beam function**

Impact-parameter space approach: SCET/TMD formulation

Analogue factorisation formula in SCET/TMD formulation

[Becher, Neuber 2011]

$$\frac{d\sigma^{(sing)}}{dQ^2 dY dp_T} = \sum_c \frac{d\sigma^{(0)}_{c\bar{c},F}}{d\Omega} H_{c\bar{c}}(Q^2,\mu)[B_c B_{\bar{c}} S](Q^2, x_1, x_2, p_T, \mu)$$

In terms of **hard**, **beam** and **soft** functions

$$[B_c B_{\bar{c}} S] = \int \frac{d^2\vec{b}}{(2\pi)^2} e^{i\vec{b}\cdot p_T} \tilde{B}_c(x_1, b, \mu, \nu/Q) \tilde{B}_{\bar{c}}(x_2, b, \mu, \nu/Q) \tilde{S}(b, \nu, \mu)$$

$$= \int \frac{d^2\vec{b}}{(2\pi)^2} e^{i\vec{b}\cdot p_T} \tilde{f}_c^{\mathrm{TMD}}(x_1, b, \mu, \nu/Q) \tilde{f}_{\bar{c}}^{\mathrm{TMD}}(x_2, b, \mu, \nu/Q)$$

Resummation follows from solving factorization properties in the singular region and associated RGE

Whenever there is **factorization**, there is **evolution**; wherever there is **evolution**, there is **resummation** (G. Sterman)

Direct space approach

Direct-space resummation in the RadISH formalism is based on a physical picture in which hard particles incoming to a primary scattering coherently radiate an ensemble of soft and collinear partons

[Monni, Re, Torrielli 2016, Bizon, Monni, Re, LR, Torrielli 2017]

$$\frac{d\sigma^{(sing)}(p_T)}{d\Phi_B} = \int dp_T \frac{d\sigma^{\text{sing}}}{dp_T d\Phi_B} = \int \frac{dk_{t1}}{k_{t1}} \mathscr{L}(k_{t1}) e^{-R(k_{t1})} \mathscr{F}(p_T, \Phi_B, k_{t1})$$

$$\mathscr{L}(k_{t1}) = \sum_{c\bar{c}} |\mathscr{M}_B|^2_{c\bar{c}} \sum_{i,j} [C_{ci} \otimes f_i(k_{t1})](x_1)[C_{\bar{c}j} \otimes f_j(k_{t1})](x_2) H$$

Collinear and hard functions

$$R(k_{t1}) = \int_{k_{t1}}^{m_{\ell\ell}} \frac{dq}{q} [A(\alpha_s(q)) \ln \frac{m^2_{\ell\ell}}{Q^2} + B(\alpha_s(q^2))]$$

Universal **Sudakov radiator:** exponentiation of soft-collinear emissions

Logarithmic accuracy defined in terms of $L = \ln(k_{t,1}/m_{\ell\ell})$

Resummation: logarithmic counting

	Boundary conditions	Anomalous dimensions γ_i	Anomalous dimensions Γ_{cusp}, β	FO matching
LL	1	-	1-loop	-
NLL	1	1-loop	2-loop	-
NLL′+NLO	α_s	1-loop	2-loop	α_s
NNLL+NLO	α_s	2-loop	3-loop	α_s
NNLL′+NNLO	α_s^2	2-loop	3-loop	α_s^2
N^3LL+NNLO	α_s^2	3-loop	4-loop	α_s^2
N^3LL′+N^3LO	α_s^3	3-loop	4-loop	α_s^3
N^4LL+N^3LO	α_s^3	4-loop	5-loop	α_s^3

All ingredients at N^3LL′ now known, with partial N^4LL information available

[G. Falcioni, F. Herzog, S. Moch, and A. Vogt]
[Moch, B. Ruijl, T. Ueda, J. Vermaseren, and A. Vogt]
[J. M. Henn, G. P. Korchemsky, and B. Mistlberger]
[C. Duhr, B. Mistlberger, and G. Vita]

Resummation: gallery

N^{3}LL′/aN^{4}LL results published in recent years by many groups using various formulations

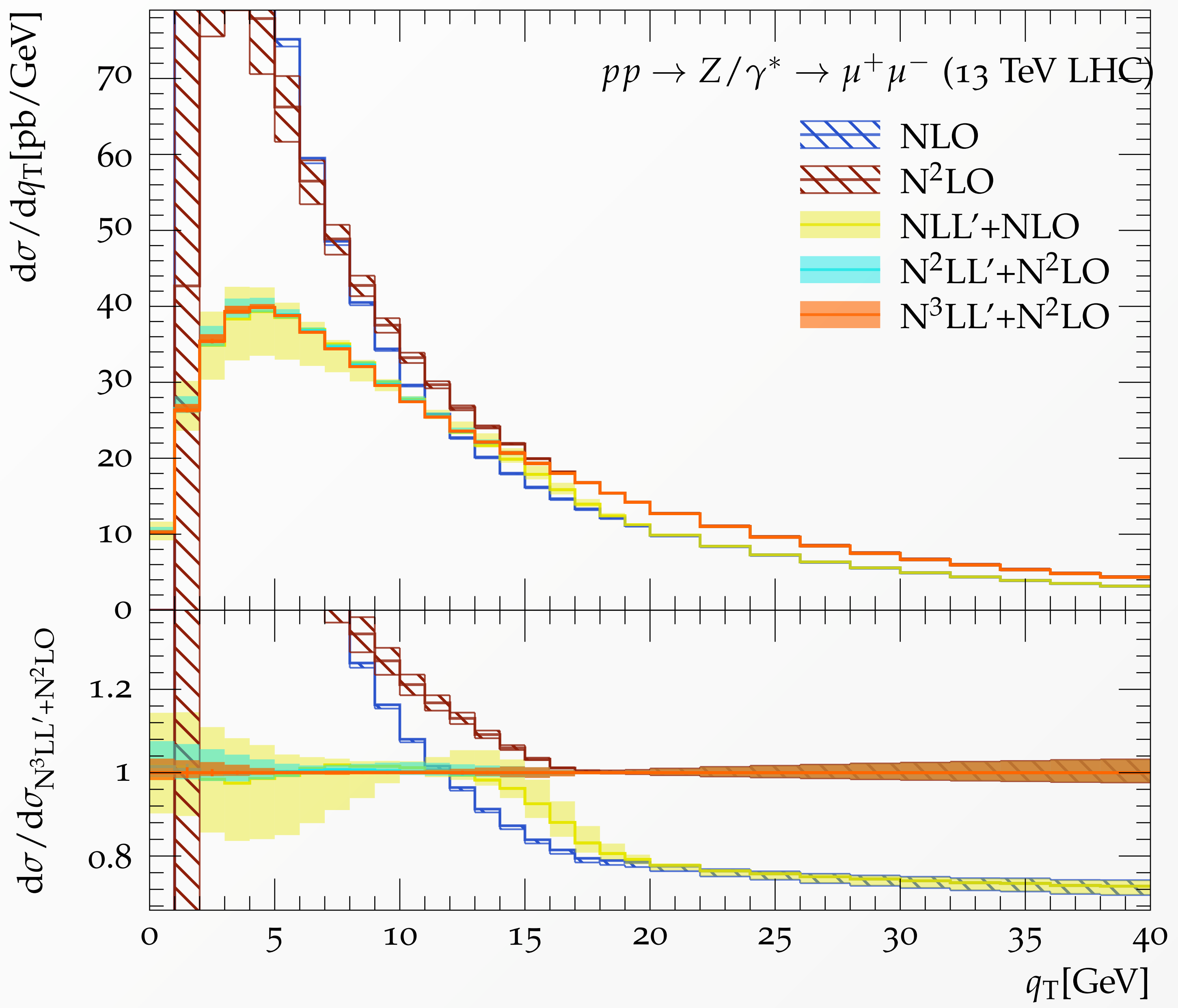

SCET formalism
[Ju, Schoenherr 2021]

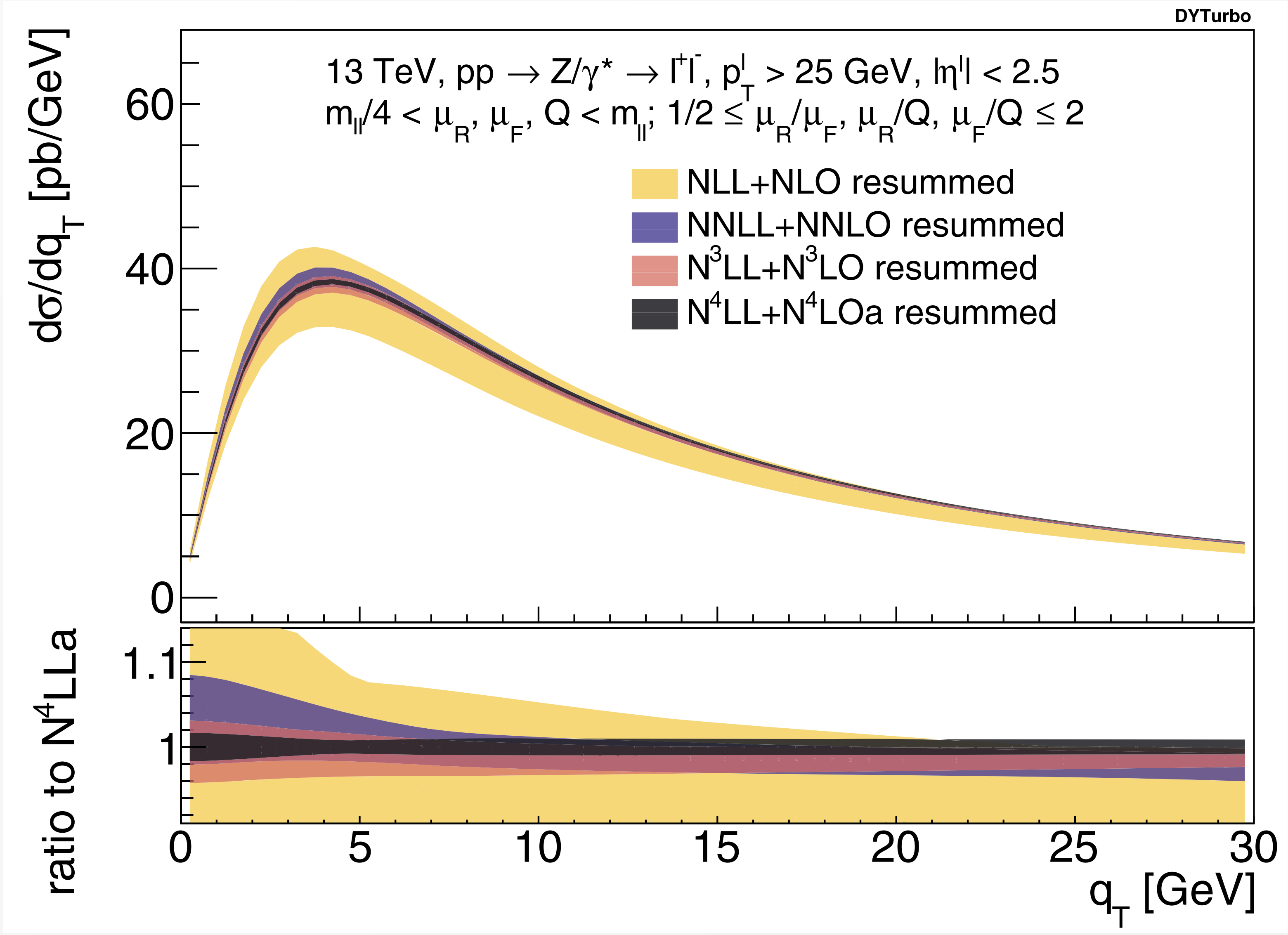

dQCD approach (DYTurbo)
[Camarda, Cieri, Ferrera 2023]

TMD framework (ARTEMIDE)
[Moos, Scimemi, Vladimirov, Zurita 2023]

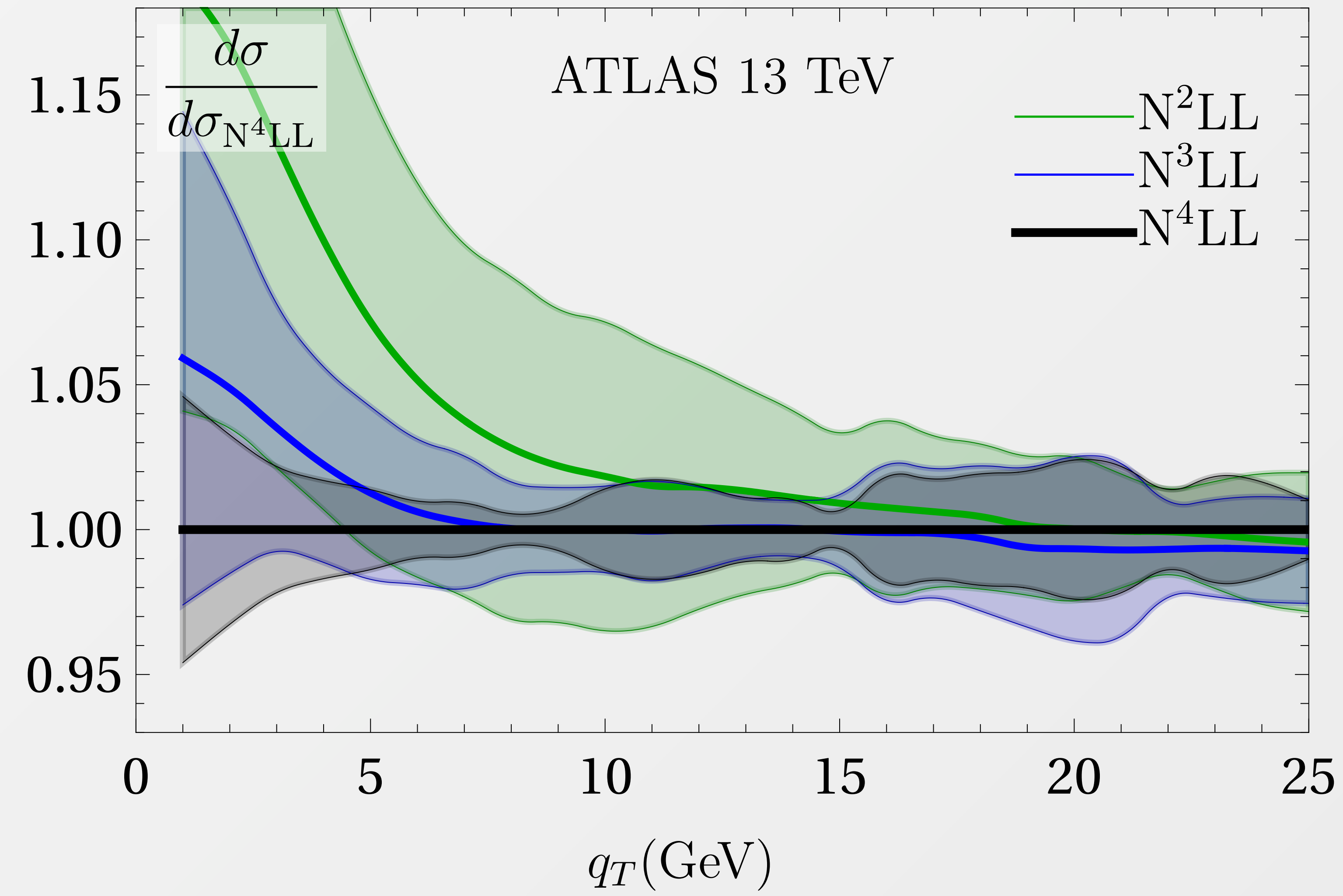

also available in SCETLIB (SCET), NangaParbat (TMD)

Matching fixed order and resummed calculations

Matching necessary to allow for a precise description across the whole p_T spectrum: **subtract** all logarithms from fixed order calculation and replace them with their **all-order summation**

Numerically challenging: need $<\%$ control of fixed order component to ensure cancellation

Several strategies to ensure that resummation does not affect the hard region of the spectrum when matching is performed, e.g. **modified logarithms**

$$\ln(Q/k_{t1}) \to \frac{1}{p} \ln\left(1 + \left(\frac{Q}{k_{t1}}\right)^p\right)$$

(restrict the rapidity phase space at large k_t)

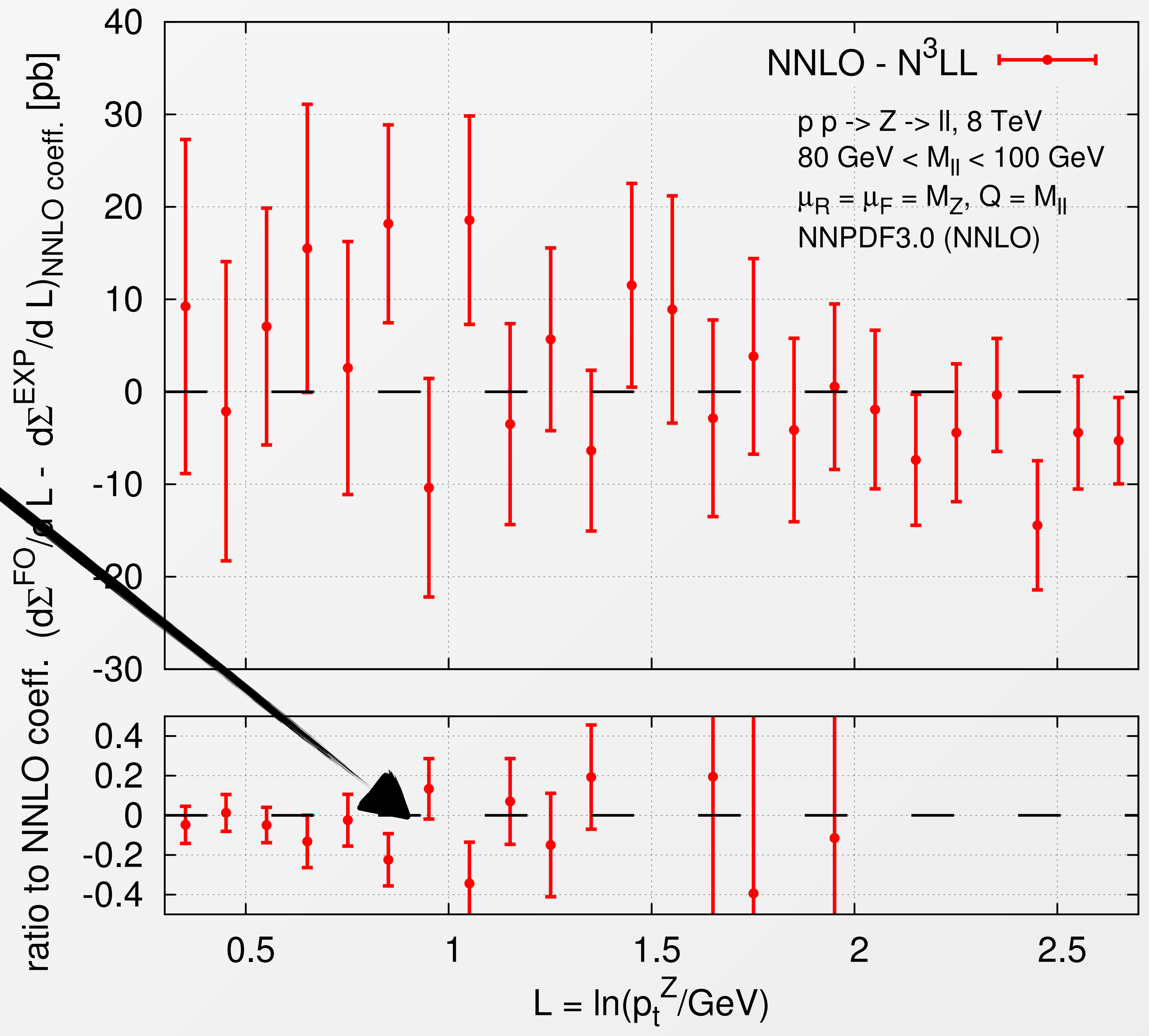

Alternative approaches use different prescriptions for turning off resummation (**profile functions**, **transition functions**…), with associated uncertainty

Precise description of the transverse momentum spectra

State-of-the-art predictions achieve N^{3}LL′/aN^{4}LL+N^{3}LO accuracy

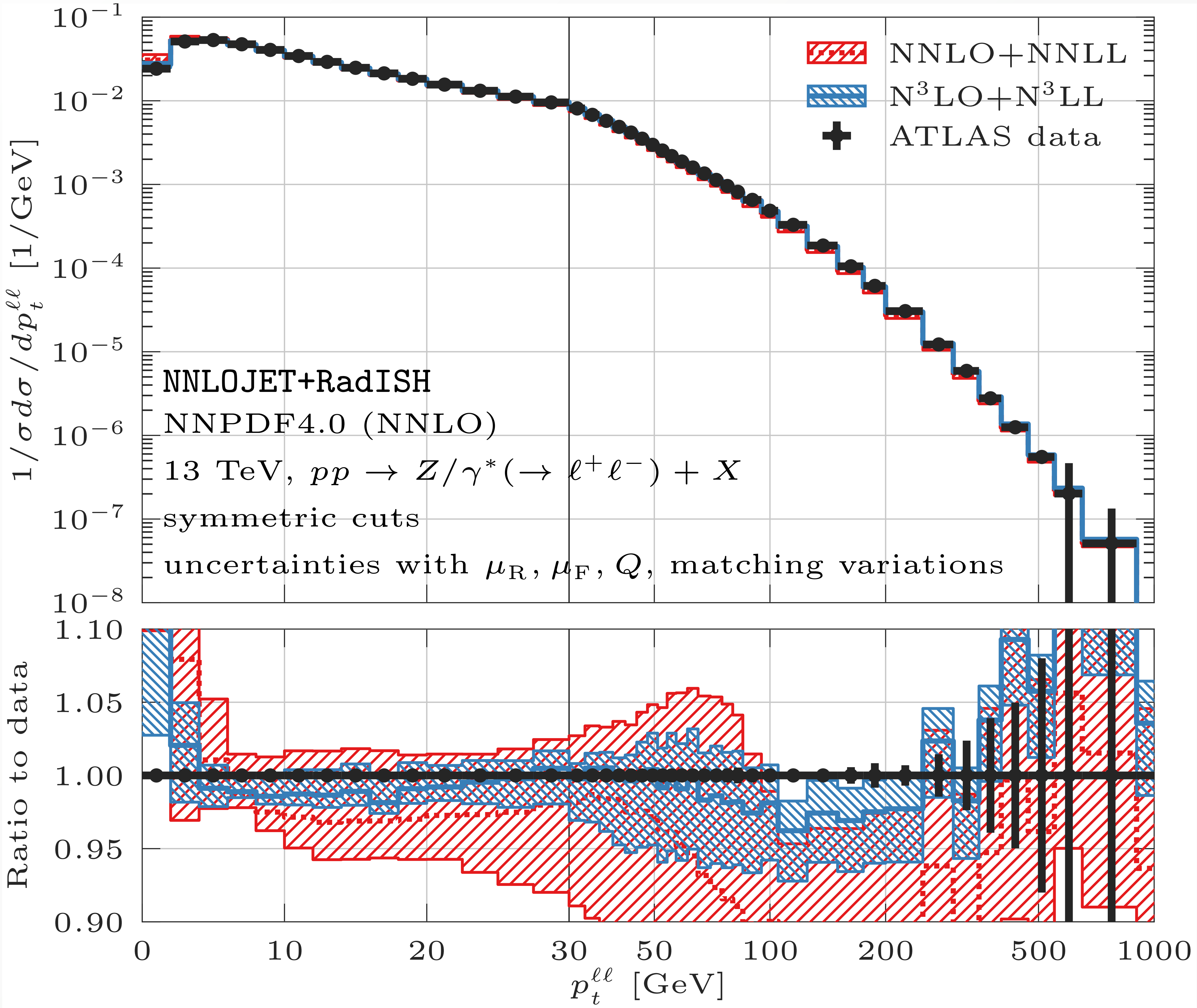

direct-space approach (RadISH)

[Chen, Gehrman, Glover, Huss, Monni, Re, LR, Torrielli 2022]

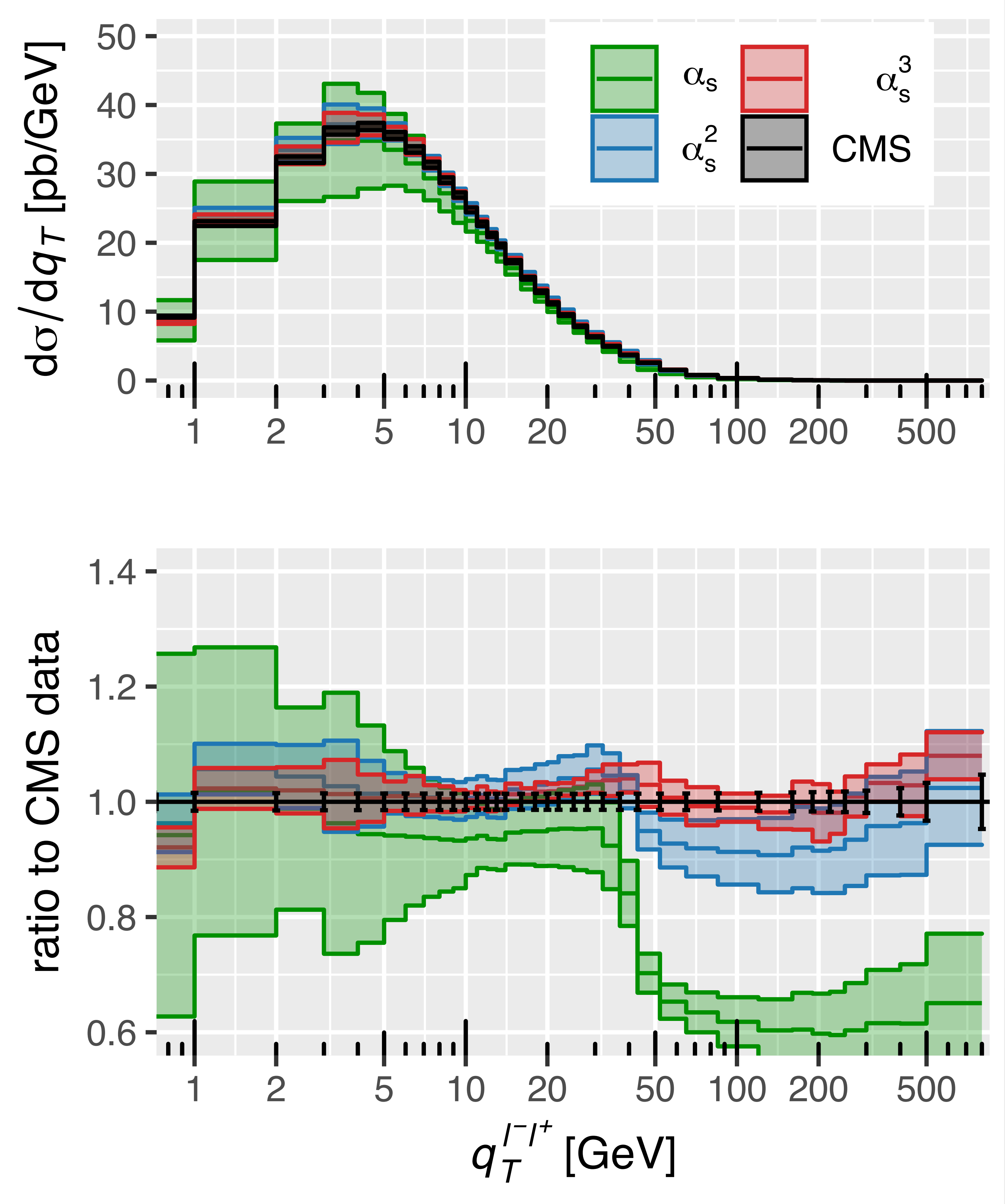

SCET formalism (Cute-MCFM)

[Neumann, Campbell 2022]

Excellent description of experimental data, with **residual scale uncertainties at the few % level**

Comparison with ATLAS data

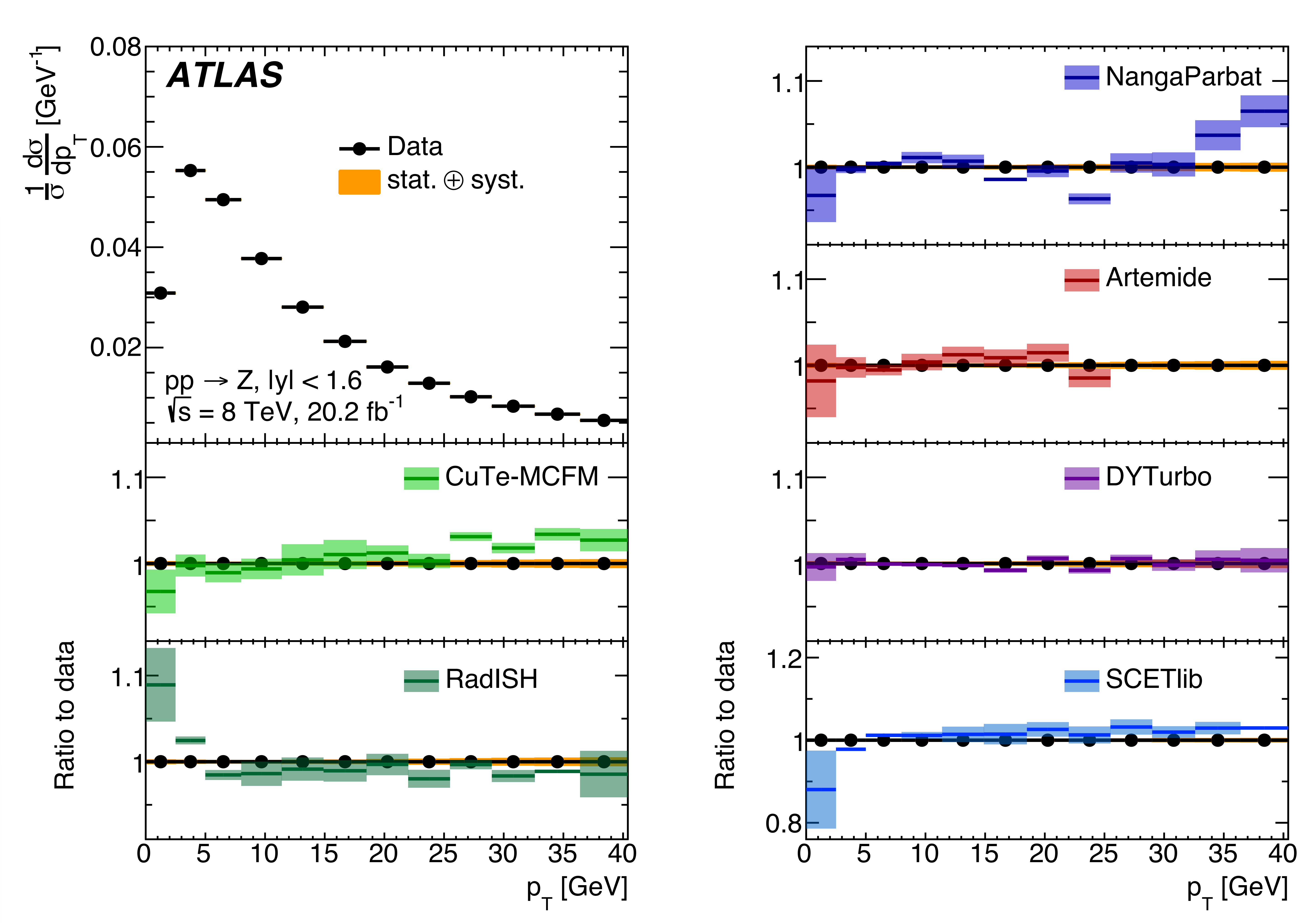

Comparison with ATLAS data at 8 TeV with different codes shows **overall good description of the data** at low transverse momentum, but highlights **some differences between alternative approaches**

Comparison with ATLAS data

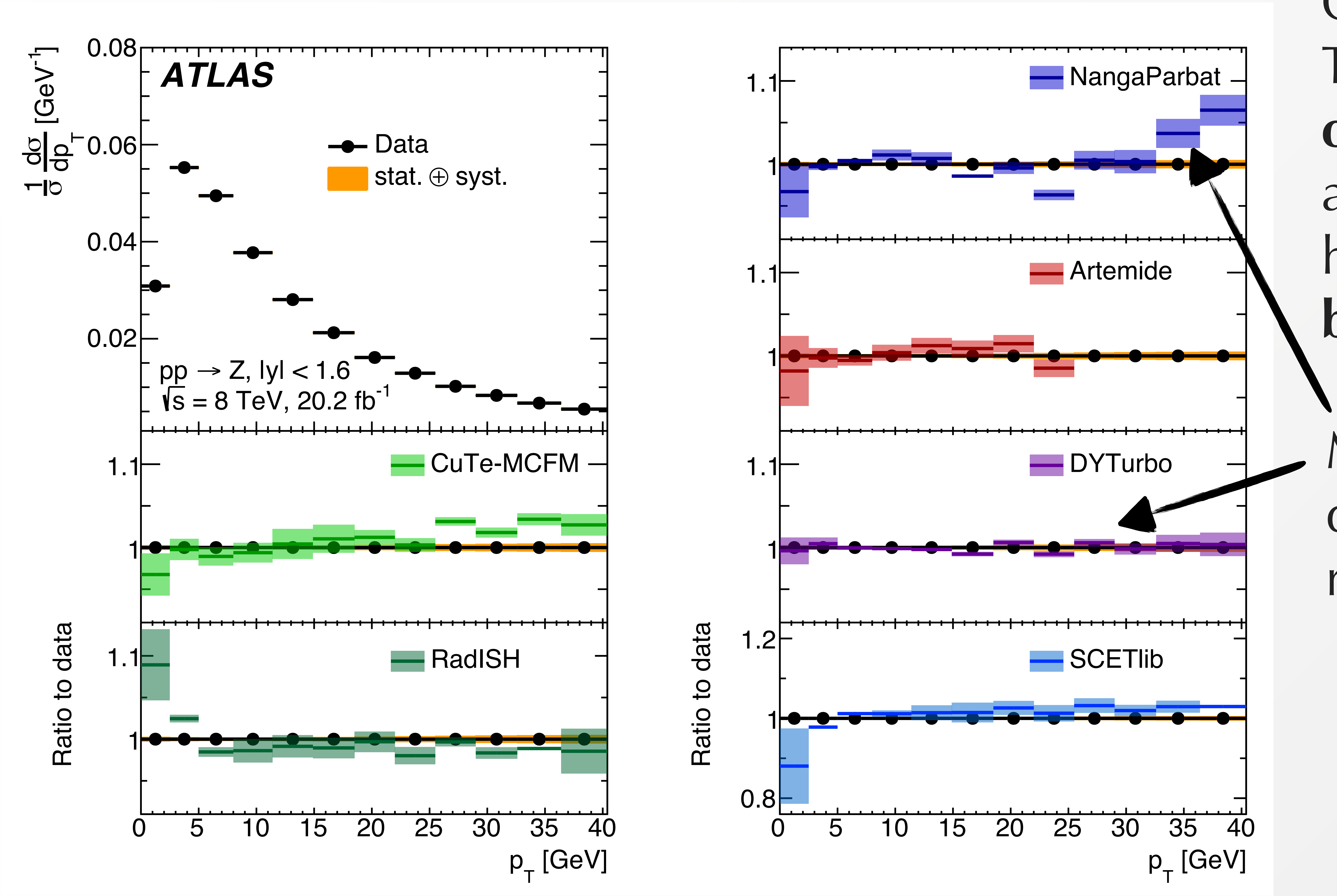

Comparison with ATLAS data at 8 TeV with different codes shows **overall good description of the data** at low transverse momentum, but highlights **some differences between alternative approaches**

Matching ambiguities affect description of data in the transition region

Comparison with ATLAS data

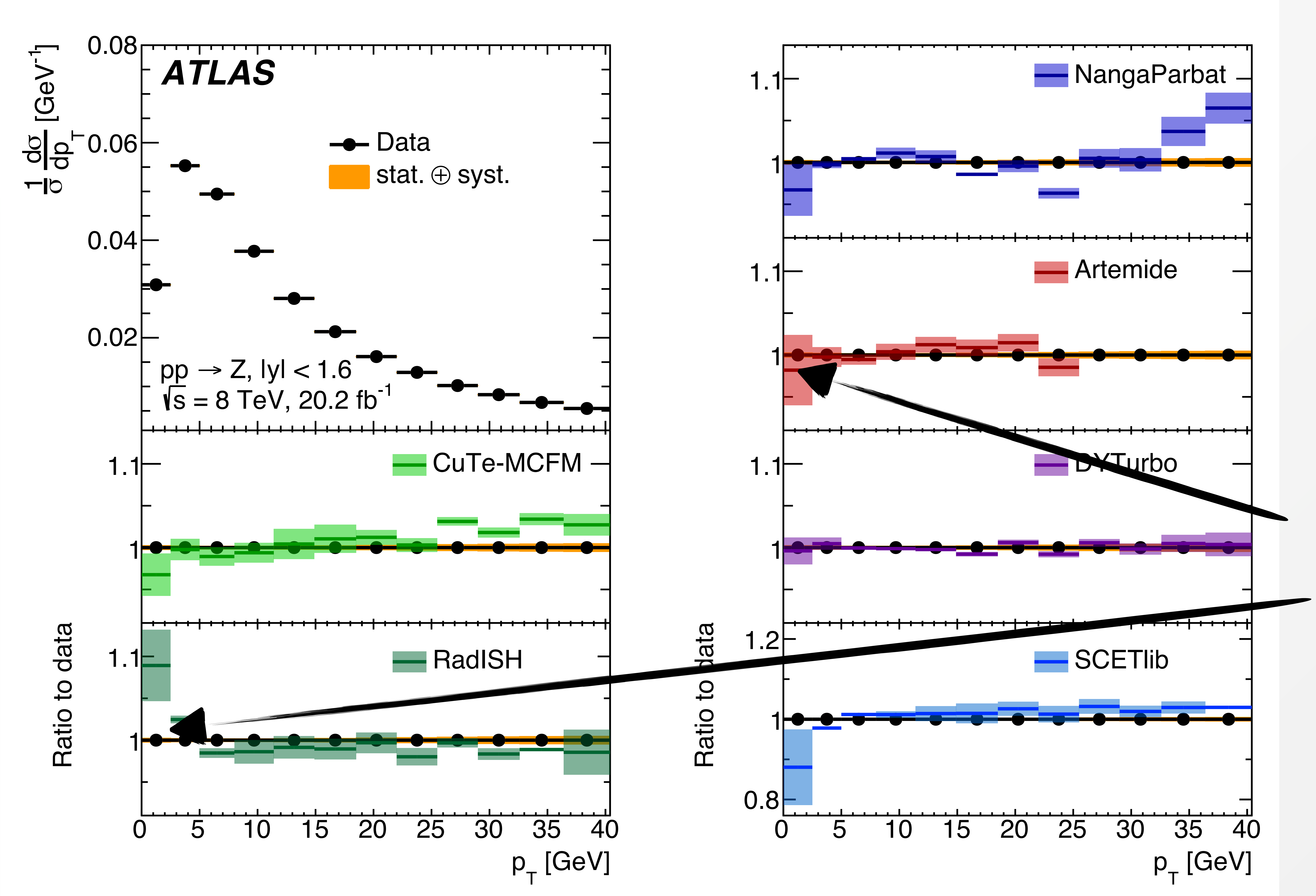

Comparison with ATLAS data at 8 TeV with different codes shows **overall good description of the data** at low transverse momentum, but highlights **some differences between alternative approaches**

Description at low transverse momentum affected by the inclusion of (tuned) NP corrections, absent in some formalisms

Comparison with ATLAS data

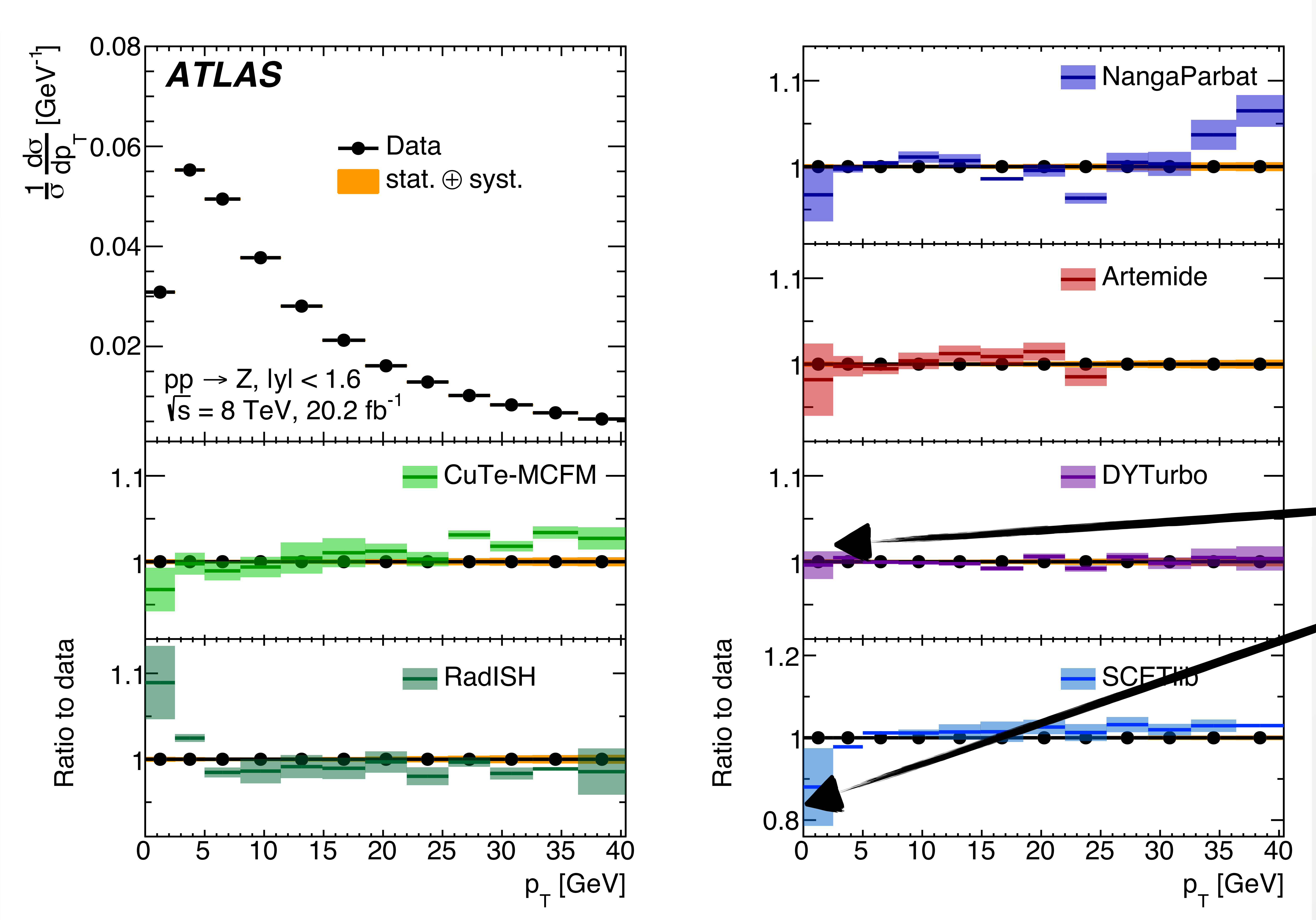

Comparison with ATLAS data at 8 TeV with different codes shows **overall good description of the data** at low transverse momentum, but highlights **some differences between alternative approaches**

Estimate of missing higher-order corrections can vary significantly among different approaches

Comparison with ATLAS data

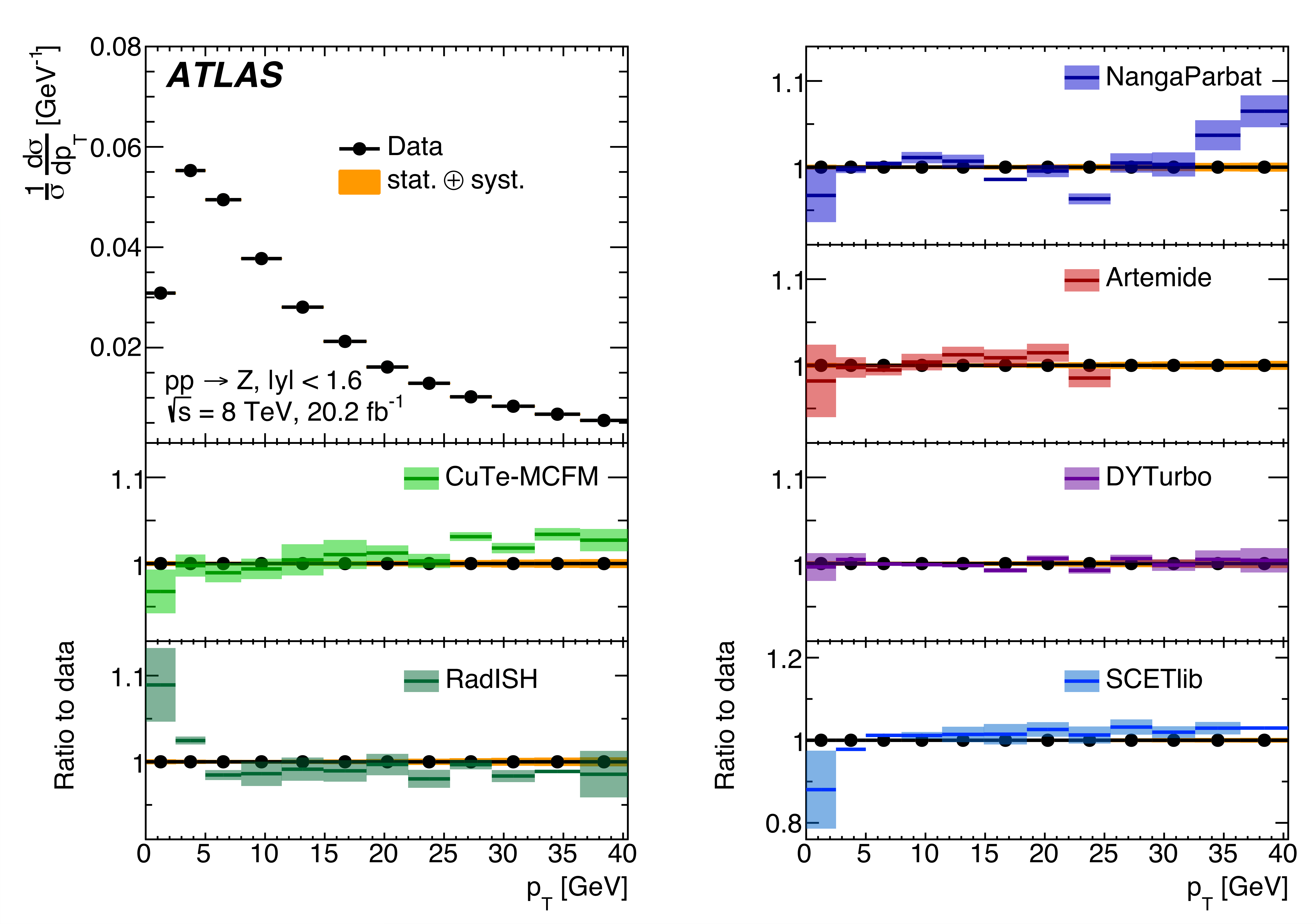

Comparison with ATLAS data at 8 TeV with different codes shows **overall good description of the data** at low transverse momentum, but highlights **some differences between alternative approaches**

Motivates benchmark of resummed calculations to address and understand these differences

Benchmark: settings

Benchmark on three levels:

Level 1:

- Pure resummed predictions at $Q = m_Z$, $Y = 0$, MSHT20 NNLO PDFs
- Nominal logarithms to ensure consistency, central scales; no NP corrections

Level 2:

- Still only resummed piece
- Each group uses their default settings for scales, resummation turn-off, etc

Level 3:

- Includes matching to fixed order, possible inclusion of NP corrections

Final goal: comparison with 8 TeV ATLAS data with agreed benchmark settings

Benchmark: status

Ongoing effort: currently moving to level 3 predictions for all groups involved, preparing draft

Predictions at level 3 already available from Cute-MCFM, RadISH, SCETLIB with final settings. Other groups in the process of uploading their final predictions

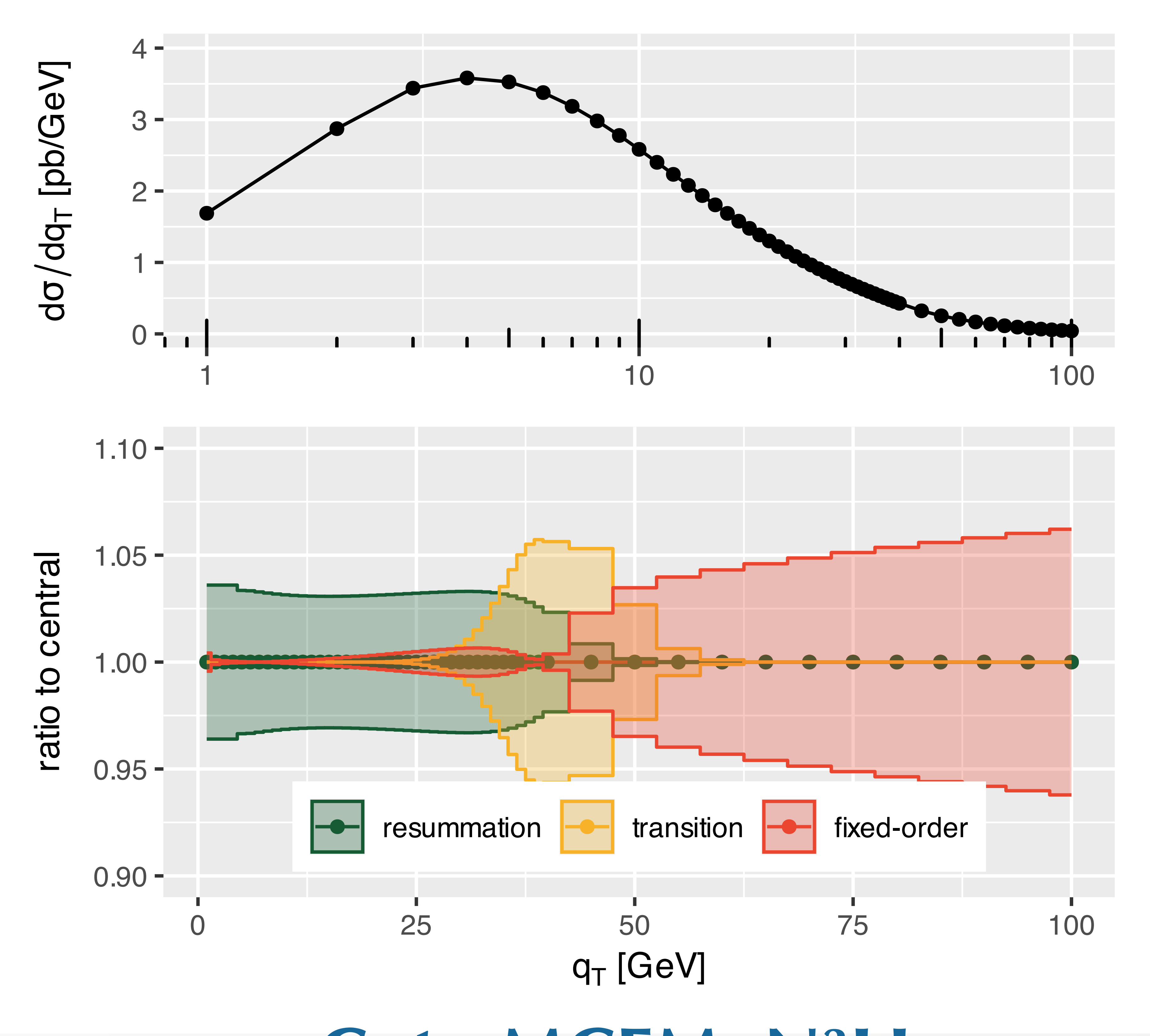

Cute-MCFM, N^3LL

First sections almost complete, sections for each level will be written once all results are available

Individual groups working on their respective appendices

Many lessons learned, see slides by J. Michel, T. Cridge, T. Neumann in past general EWWG meetings

Benchmark: example of lesson learned

Level 1 predictions showed overall percent agreement between different codes, but highlighted difference at low p_T between different approaches

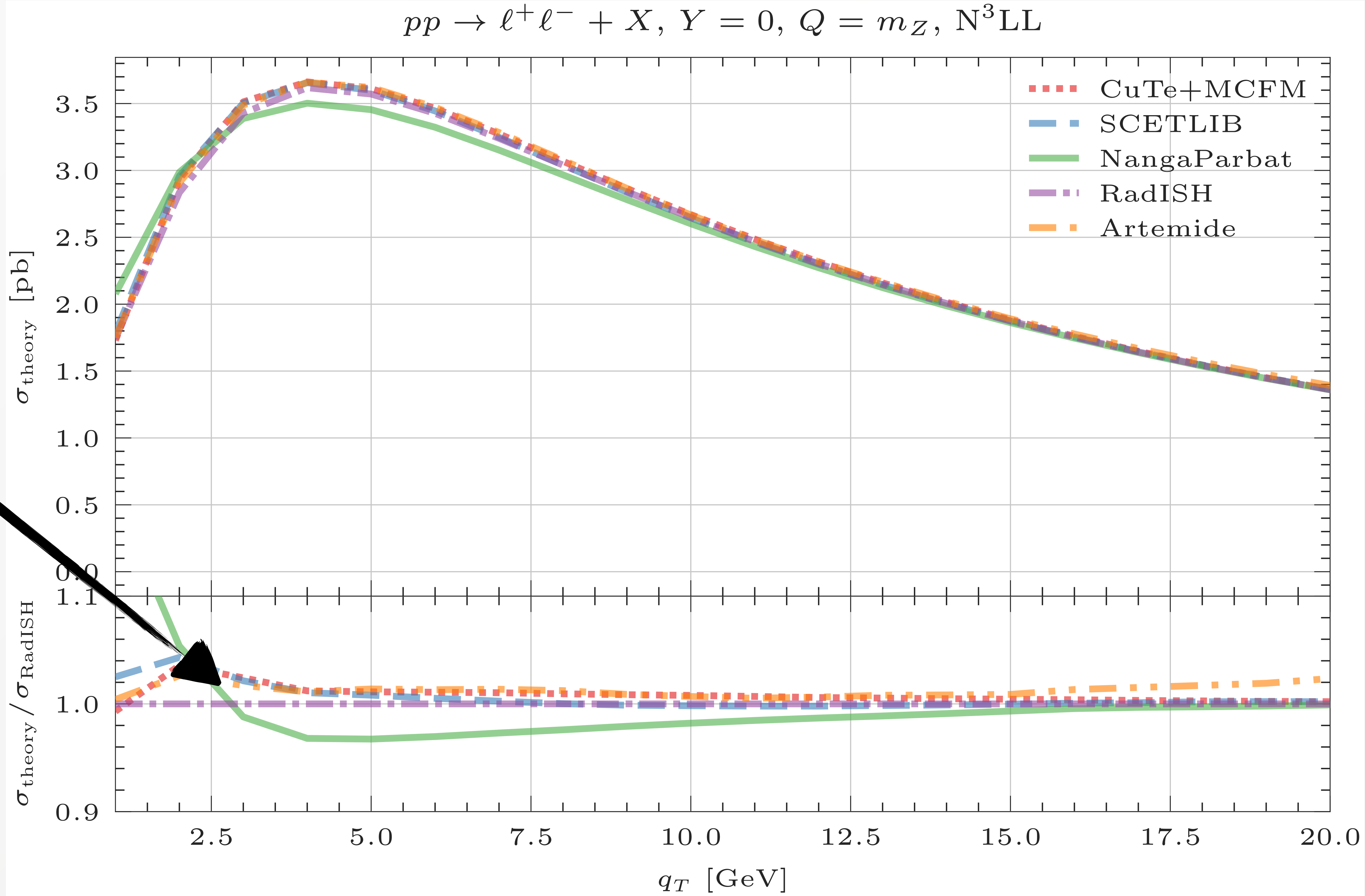

Benchmark: example of lesson learned

Level 1 predictions showed overall percent agreement between different codes, but highlighted difference at low p_T between different approaches

Differences related to the treatment of the Landau pole in NangaParbat

"Local" (only scales) vs. "Global" (everywhere) implementation of $b*$ prescription

$$b* = \frac{b}{\sqrt{1 + (b/b_{\text{lim}})}}, \quad b* < b_{\text{lim}}$$

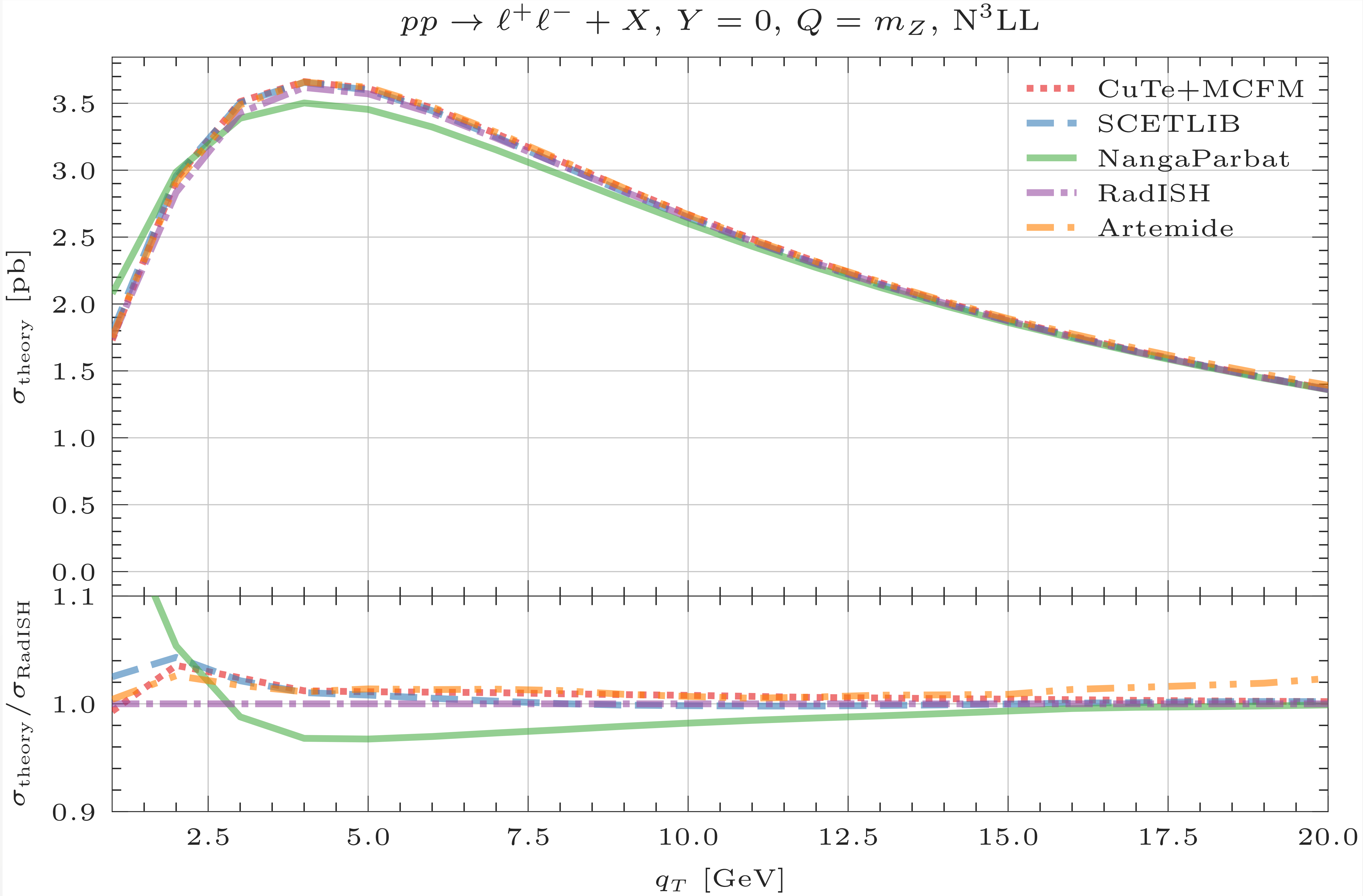

Benchmark: example of lesson learned

Level 1 predictions showed overall percent agreement between different codes, but highlighted difference at low p_T between different approaches

Differences related to the treatment of the Landau pole in NangaParbat

"Local" (only scales) vs. "Global" (everywhere) implementation of $b*$ prescription

$$b* = \frac{b}{\sqrt{1 + (b/b_{\mathrm{lim}})}}, \quad b* < b_{\mathrm{lim}}$$

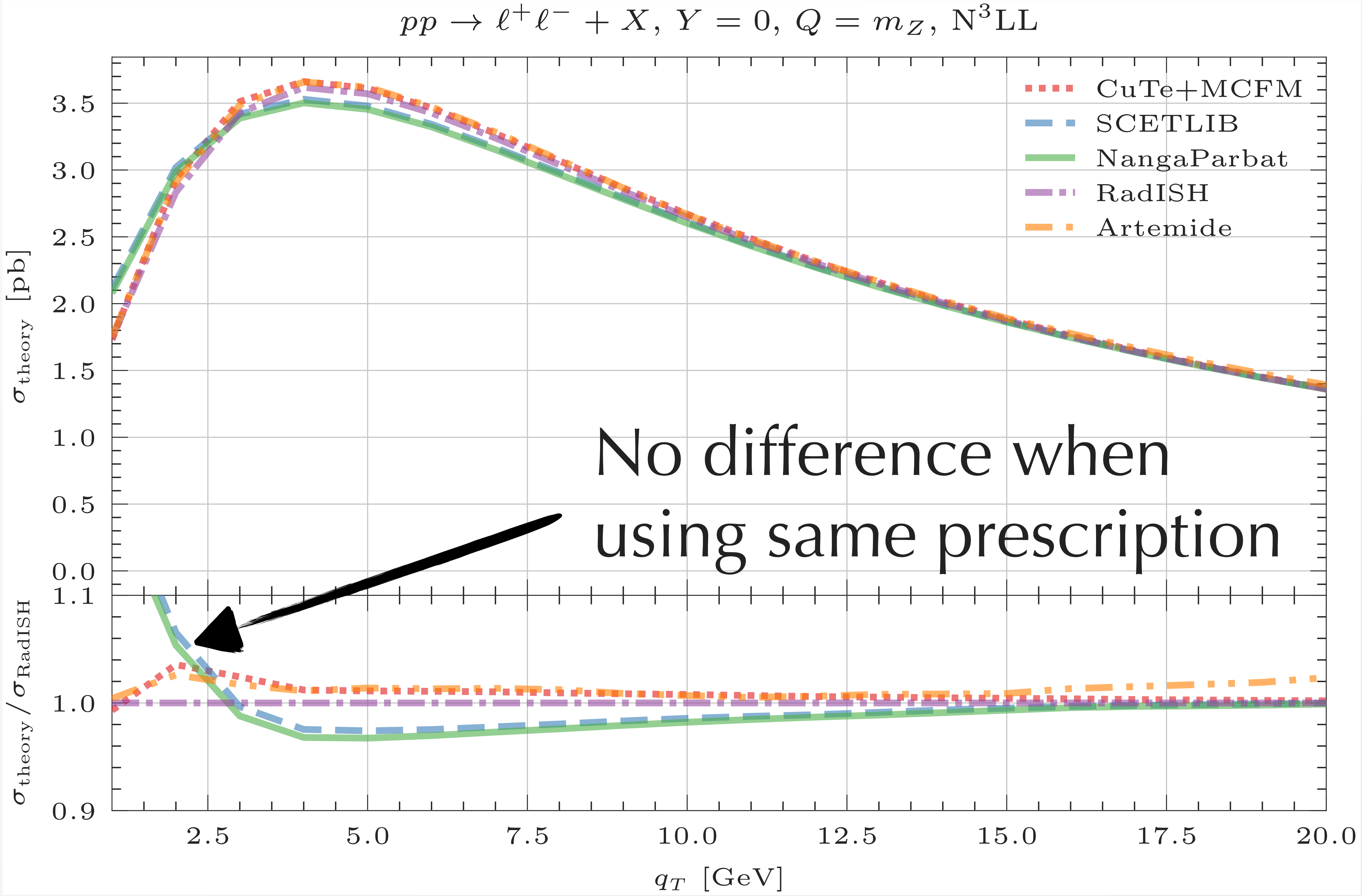

Highlights importance of understanding impact of non-perturbative corrections, even in the absence of fitted NP form factor

Non perturbative corrections and p_T^Z

Collinear factorization valid up to power corrections $\mathcal{O}(\Lambda^n_{\mathrm{QCD}}/Q^n)$

In principle, easy to imagine mechanisms for linear power corrections, which would be a disaster for precision programme at the LHC

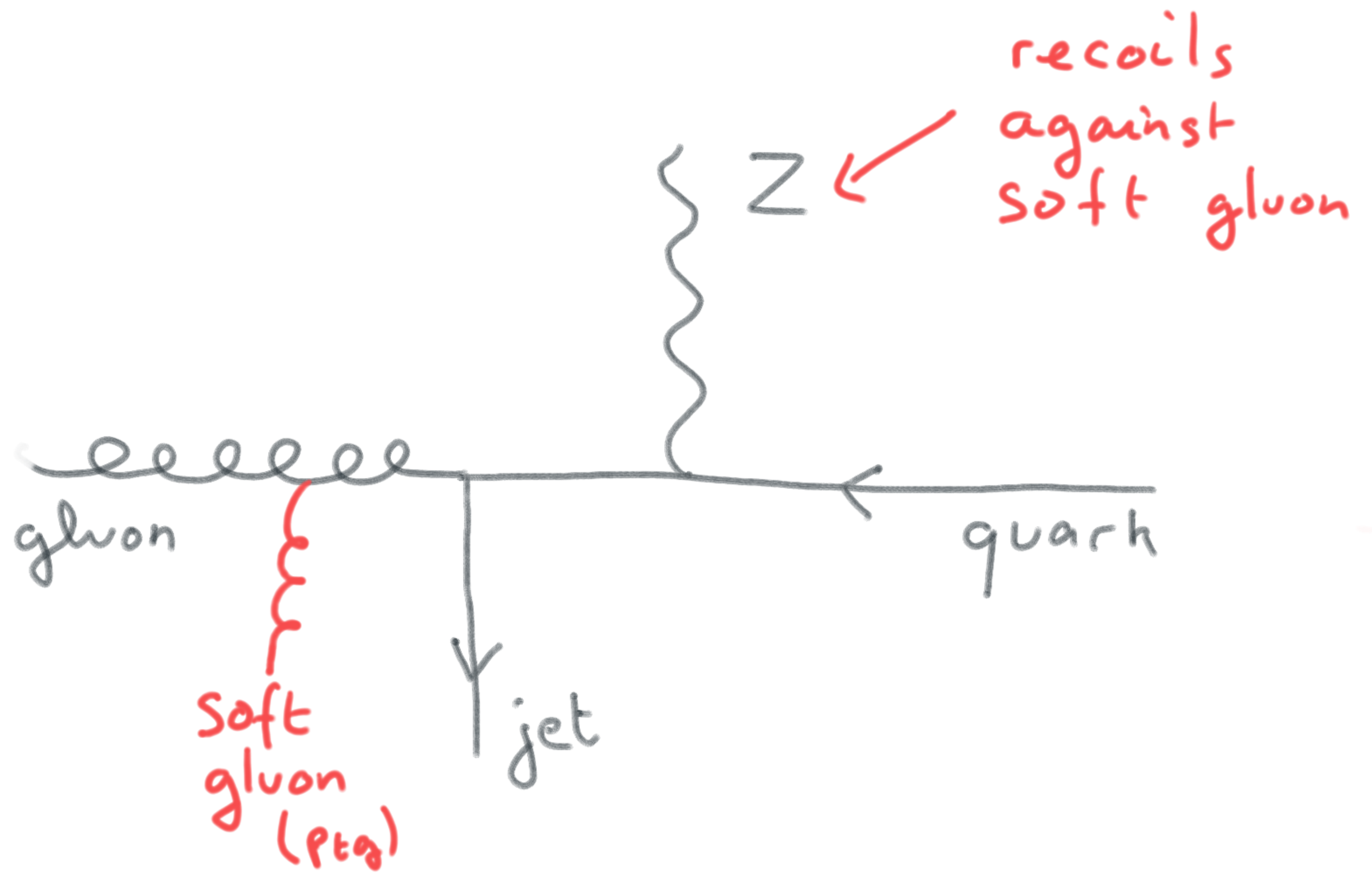

[G.P. Salam]

Linear term could be generated when integrating over soft d.o.f. which is not azimuthally symmetric

Luckily, for p_T this does not happen!

[Ravasio, Limatola, Nason 2021]

[Caola, Ravasio, Limatola, Melnikov, Nason 2022]

No linear power corrections affect the transverse momentum spectrum

Treatment of non-perturbative corrections

Nevertheless, NP corrections **can be sizeable** in the first p_T bins. Often supplemented by introducing a non-perturbative correction **determined from data**

e.g. in TMD factorisation $$\tilde{f}_c^{\mathrm{TMD}}(x_1, b, \mu, \zeta) = \tilde{f}_c^{\mathrm{NP}}(x_1, b, \mu)\tilde{f}_c^{\mathrm{TMD}}(x_1, b^*, \mu, \zeta)$$

Properties of $\tilde{f}_c^{\mathrm{NP}}(x_1, b, \mu)$ determined by TMD factorisation; function is not universal, as it depends on the **strategy used to regularise the Landau pole**

Extraction from data of the non-perturbative component to the Collins-Soper kernel can be compared with recent **lattice QCD computation**

Progress in lattice computations opens the door for future first-principles QCD predictions of the CS kernel and to possible combination with fits to data

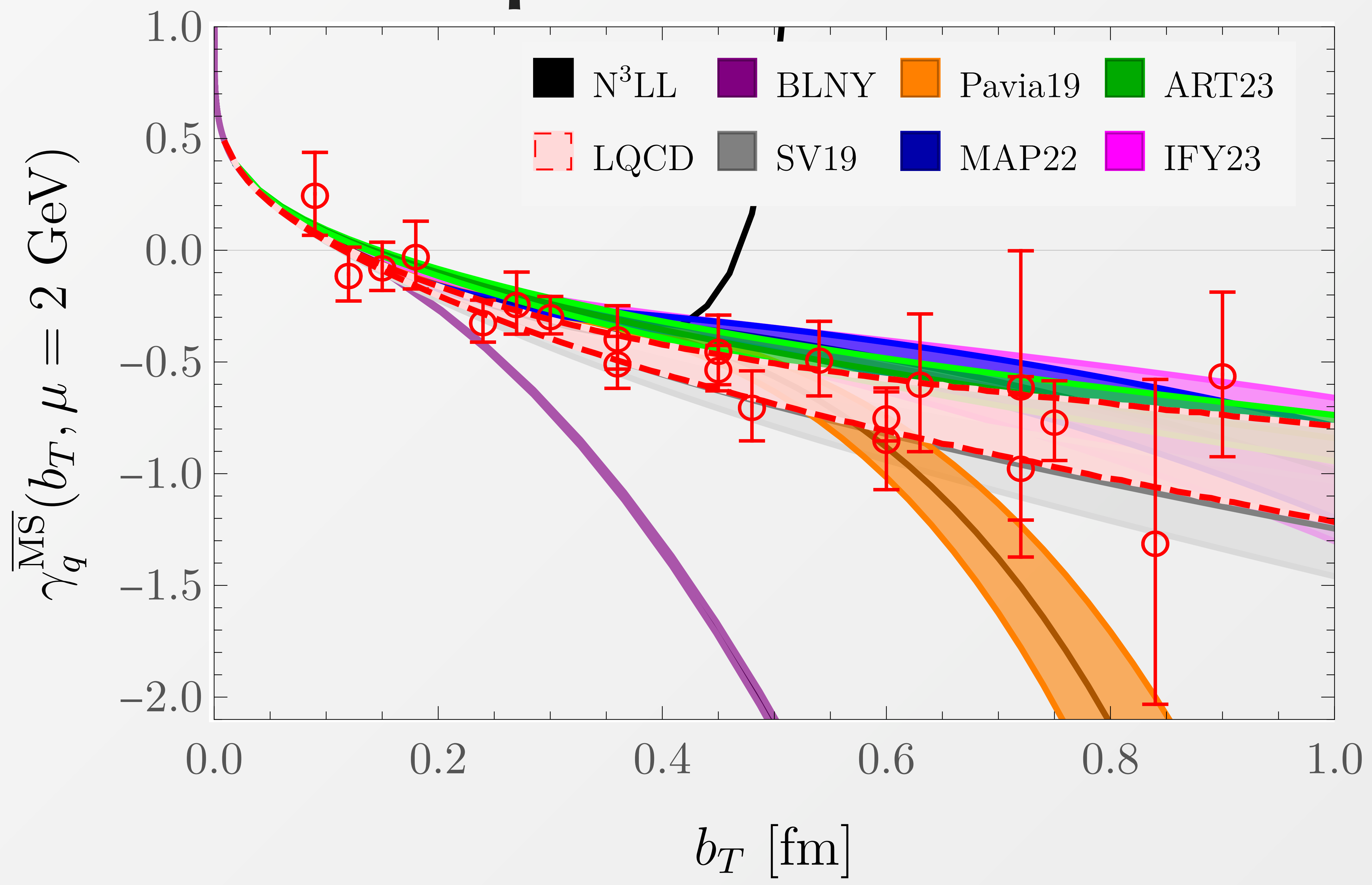

[Avkhadiev, Shanahan, Wagman, Zhao 2024]

The role of PDFs

Non negligible differences in absolute value between different groups (NNPDF, MHST)

Discrepancy explained by fitted (NNPDF) vs. perturbative (MSHT) charm and different value of the charm mass, still state-of-the-art PDFs set **can differ at the few % level**

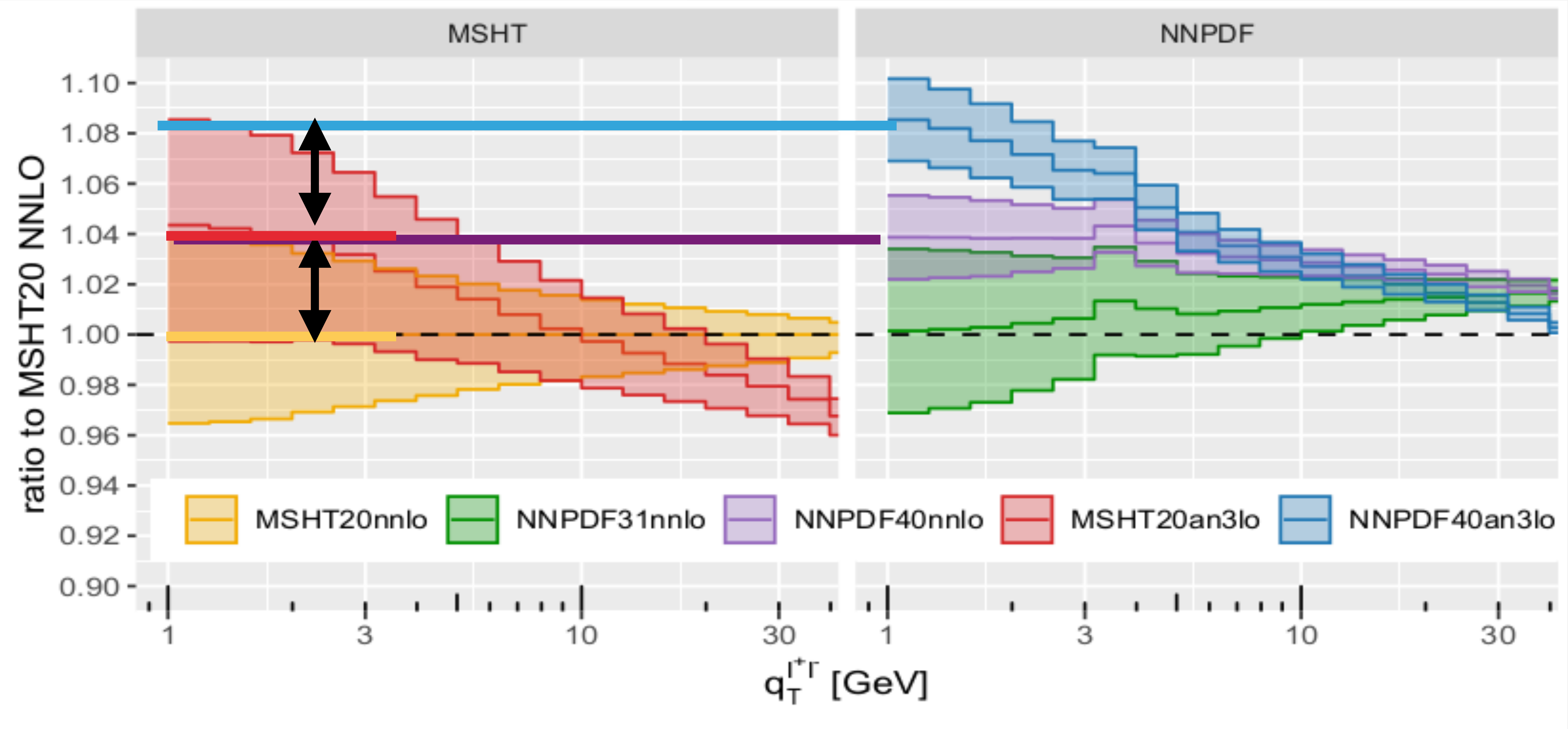

[Neumann @ Loops and Legs 2024]

The role of PDFs

Non negligible differences in absolute value between different groups (NNPDF, MHST)

Discrepancy explained by fitted (NNPDF) vs. perturbative (MSHT) charm and different value of the charm mass, still state-of-the-art PDFs set **can differ at the few % level**

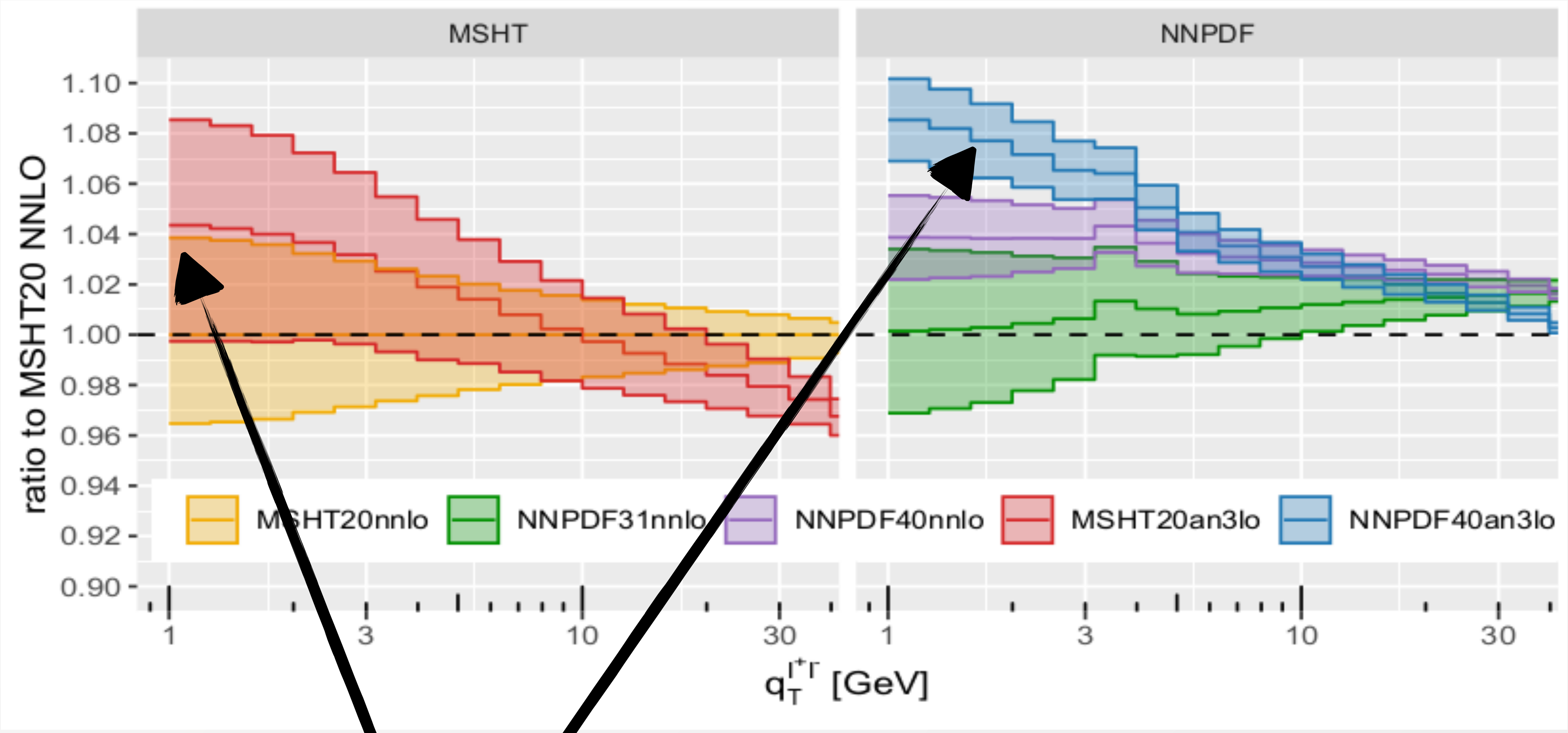

[Neumann @ Loops and Legs 2024]

aN^{3}LO PDFs from MSHT or NNPDF have a similar impact in shape on the Z p_T spectrum. Substantial differences can impact the agreement with the experimental data

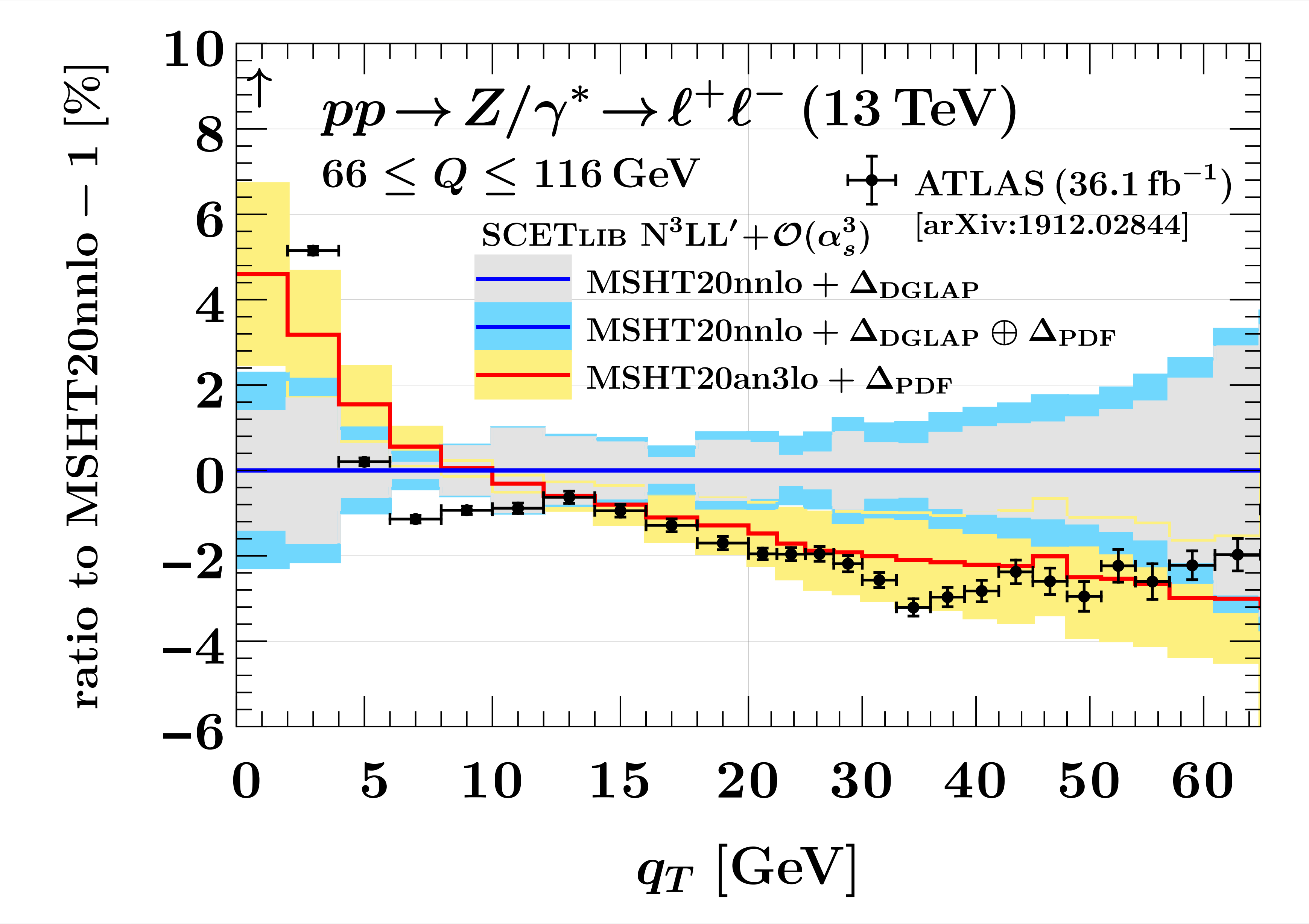

[Michel @ EW WG 2022]

Precision programme requires a deeper understanding of PDF/N^{3}LO DGLAP role for such a crucial observable

see Mandy's talk later

W and Z production: understanding correlations

Precise data on p_T^Z spectrum can be employed in measurement of m_W only indirectly, by modelling the differences between Z and W production processes

$$\frac{1}{\sigma^W}\frac{d\sigma^W}{p_\perp^W} \sim \frac{1}{\sigma^Z_{\rm data}}\frac{d\sigma^Z_{\rm data}}{p_\perp^Z}\,\frac{\frac{1}{\sigma^W_{\rm theory}}\frac{d\sigma^W_{\rm theory}}{p_\perp^W}}{\frac{1}{\sigma^Z_{\rm theory}}\frac{d\sigma^Z_{\rm theory}}{p_\perp^Z}}$$

e.g. m_W determination by ATLAS

Z and W production share a similar pattern of QCD radiative corrections, but a **precise understanding of the correlation** between the two processes is crucial to propagate consistently the information

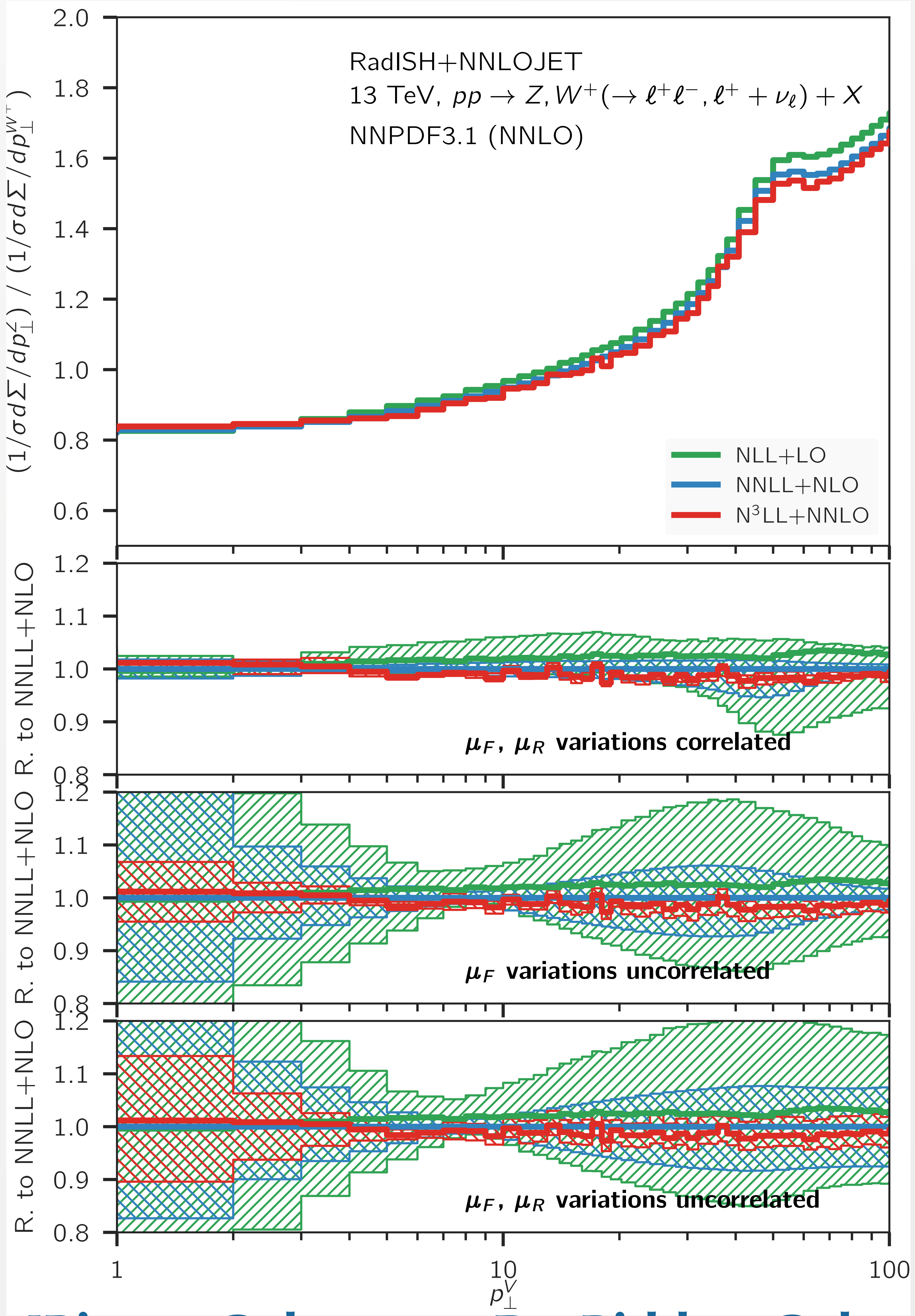

[Bizon, Gehrmann-De Ridder, Gehrmann, Glover, Huss, Monni, Re, LR, Walker '19]

The *W/Z* transverse momentum ratio: understanding correlations

Alternative uncertainty estimate: each resummation order only depends on a few semi-universal parameters: treat them as **theory nuisance parameters**

F. Tackmann, unpublished

	boundary conditions			anomalous dimensions			
order	h_n	s_n	b_n	γ_n^h	γ_n^s	Γ_n	β_n
LL	h_0	s_0	b_0	—	—	Γ_0	β_0
NLL′	h_1	s_1	b_1	γ_0^h	γ_0^s	Γ_1	β_1
NNLL′	h_2	s_2	b_2	γ_1^h	γ_1^s	Γ_2	β_2
$\text{N}^3\text{LL}'$	h_3	s_3	b_3	γ_2^h	γ_2^s	Γ_3	β_3
$\text{N}^4\text{LL}'$	h_4	s_4	b_4	γ_3^h	γ_3^s	Γ_4	β_4

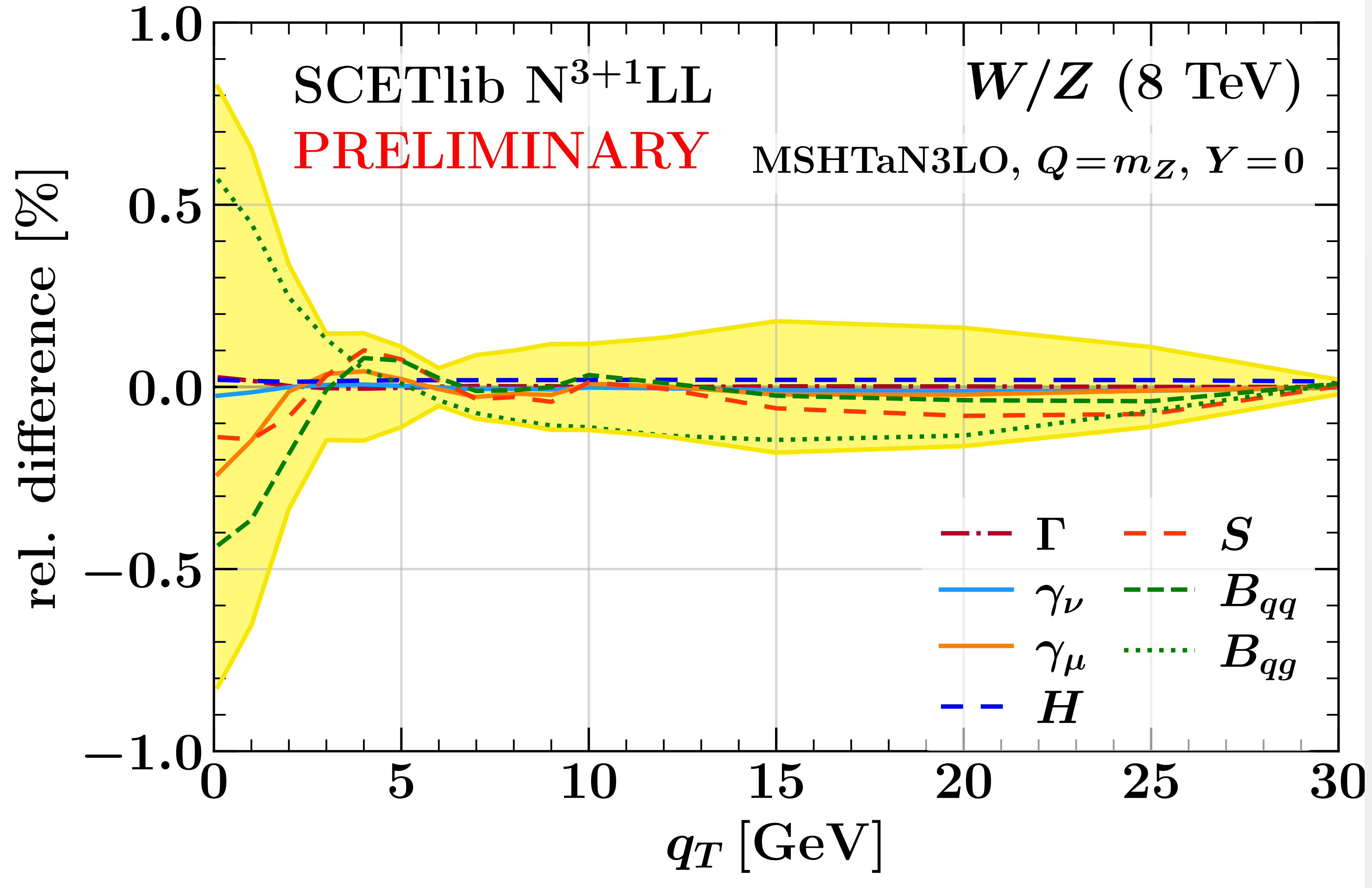

Easier to encode correlations within given assumptions, obviously not as cheap as scale variations

Transverse momentum in *W* production

Direct measurement of *W* transverse momentum would provide a direct way to test *W*/*Z* modelling and reduce the related uncertainties in a measurement of m_W

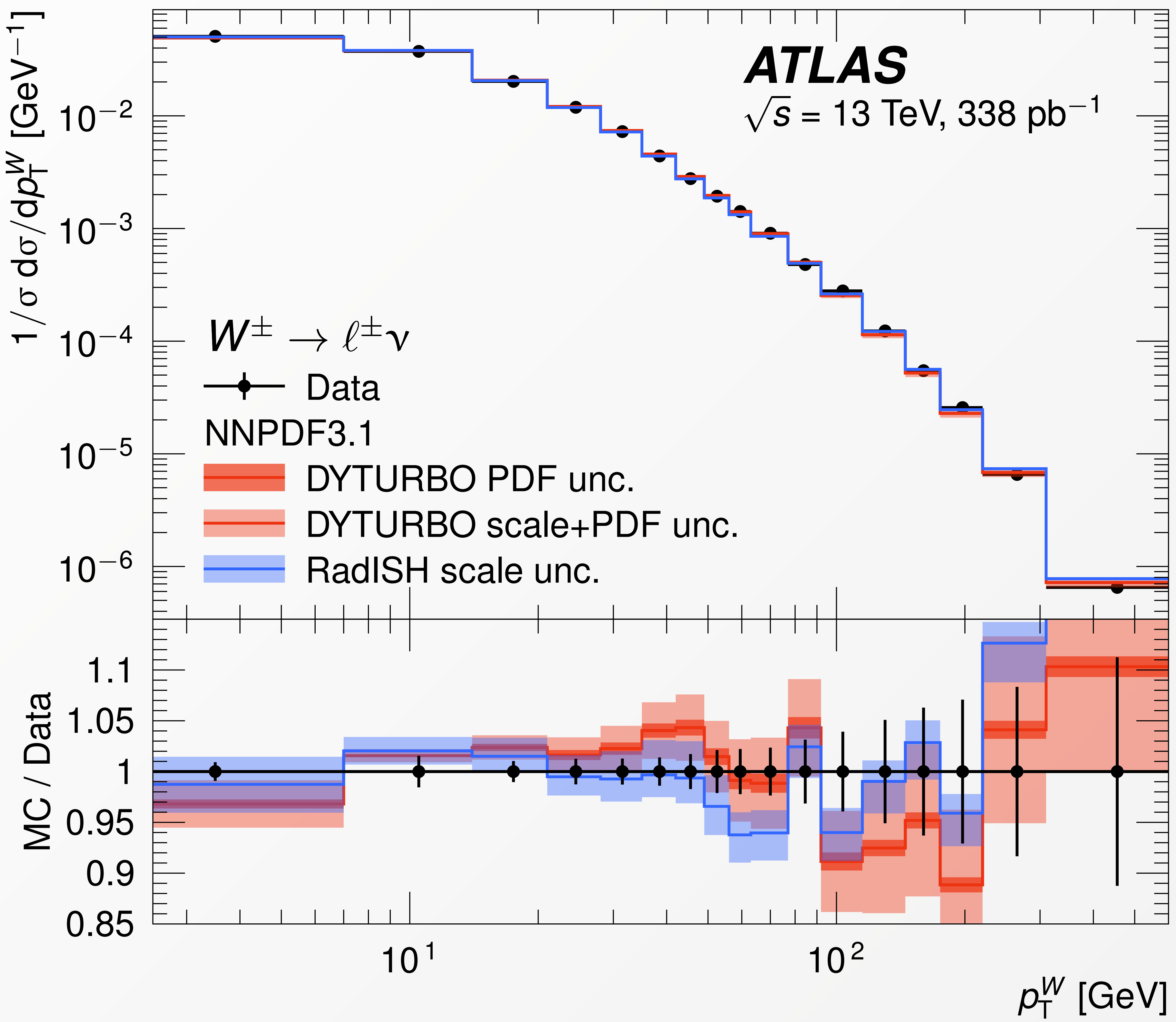

Low-pileup runs in recent ATLAS measurement show remarkable agreement with N^{3}LL+N^{3}LO (RadISH+NNLOJET) and NNLL+NNLO (DYTURBO) predictions

Transverse momentum in W production

Direct measurement of W transverse momentum would provide a direct way to test W/Z modelling and reduce the related uncertainties in a measurement of m_W

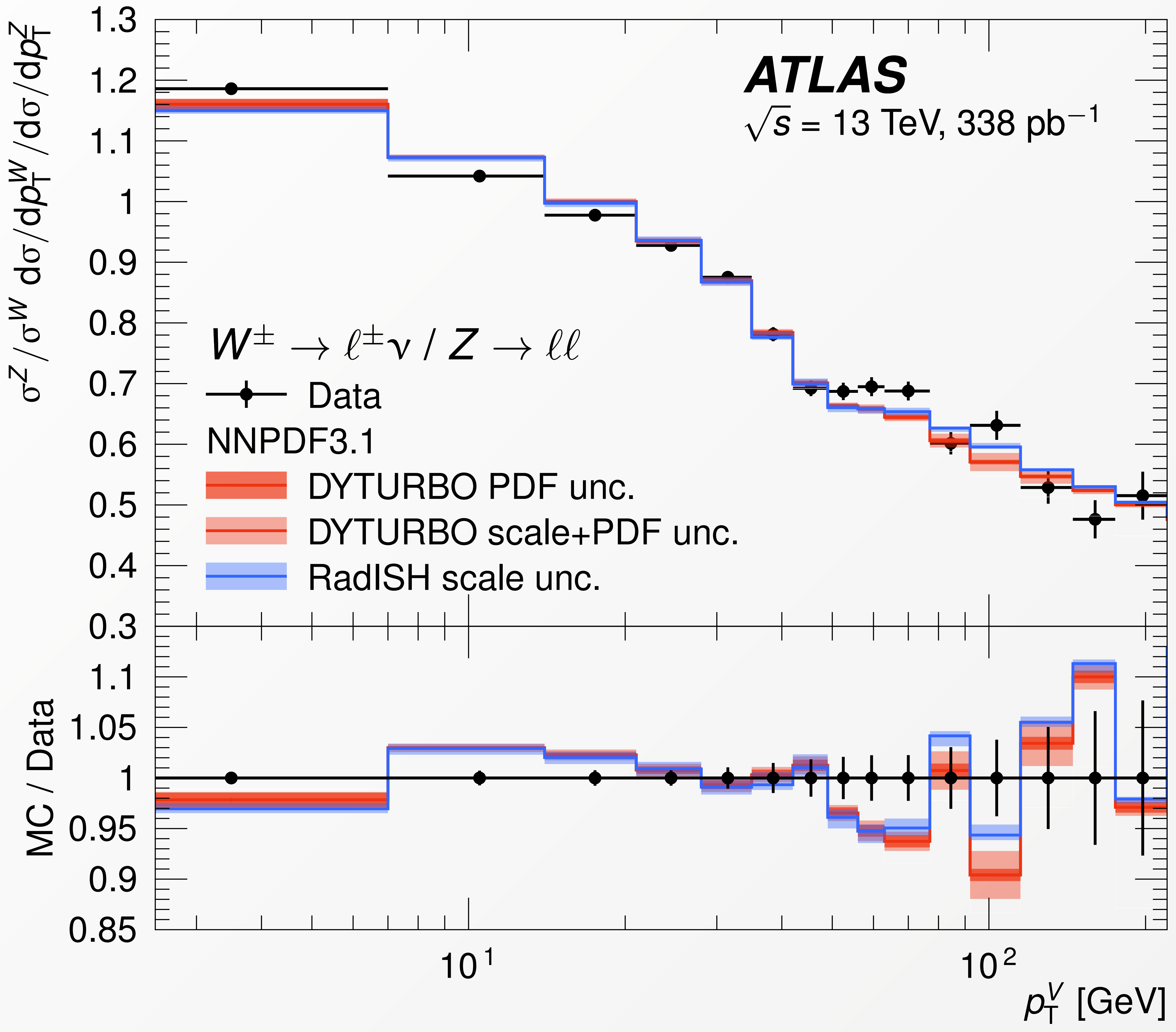

Low-pileup runs in recent ATLAS measurement show remarkable agreement with N[3]LL+N[3]LO (RadISH+NNLOJET) and NNLL+NNLO (DYTURBO) predictions

W/Z ratio is perturbatively stable but differs by a few % from the data assuming 100% correlation

Transverse momentum in *W* production

Direct measurement of *W* transverse momentum would provide a direct way to test *W/Z* modelling and reduce the related uncertainties in a measurement of m_W

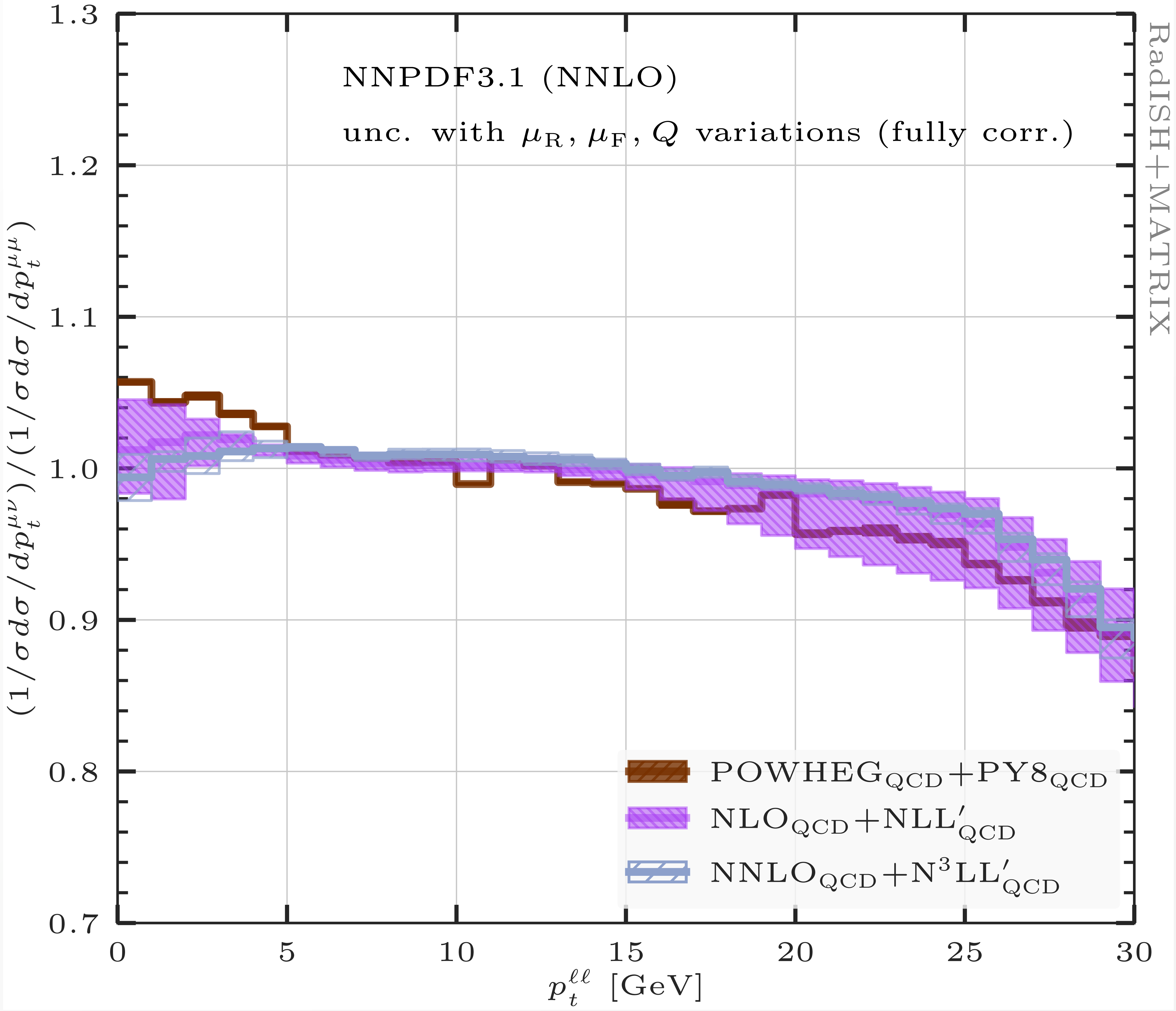

Low-pileup runs in recent ATLAS measurement show remarkable agreement with N^{3}LL+N^{3}LO (RadISH+NNLOJET) and NNLL+NNLO (DYTURBO) predictions

W/Z ratio is perturbatively stable but differs by a few % from the data assuming 100% correlation

Tuned MC predictions (POWHEG+PY8) display the same level of discrepancy and are relatively insensitive to choice of tune, intrinsic k_T, MPI and hadronisation effects

Hints towards a perturbative origin of this discrepancy

W and *Z* production: the role of EW corrections

QED and mixed QCD-EW correction patterns in *W* and *Z* production differ due to the **different number of charged legs** in NC and CC Drell-Yan production

LL QED and (factorizable) QCD/EW corrections are typically estimated by interfacing QCD Monte Carlo programs with dedicated QED shower programs, such as PHOTOS

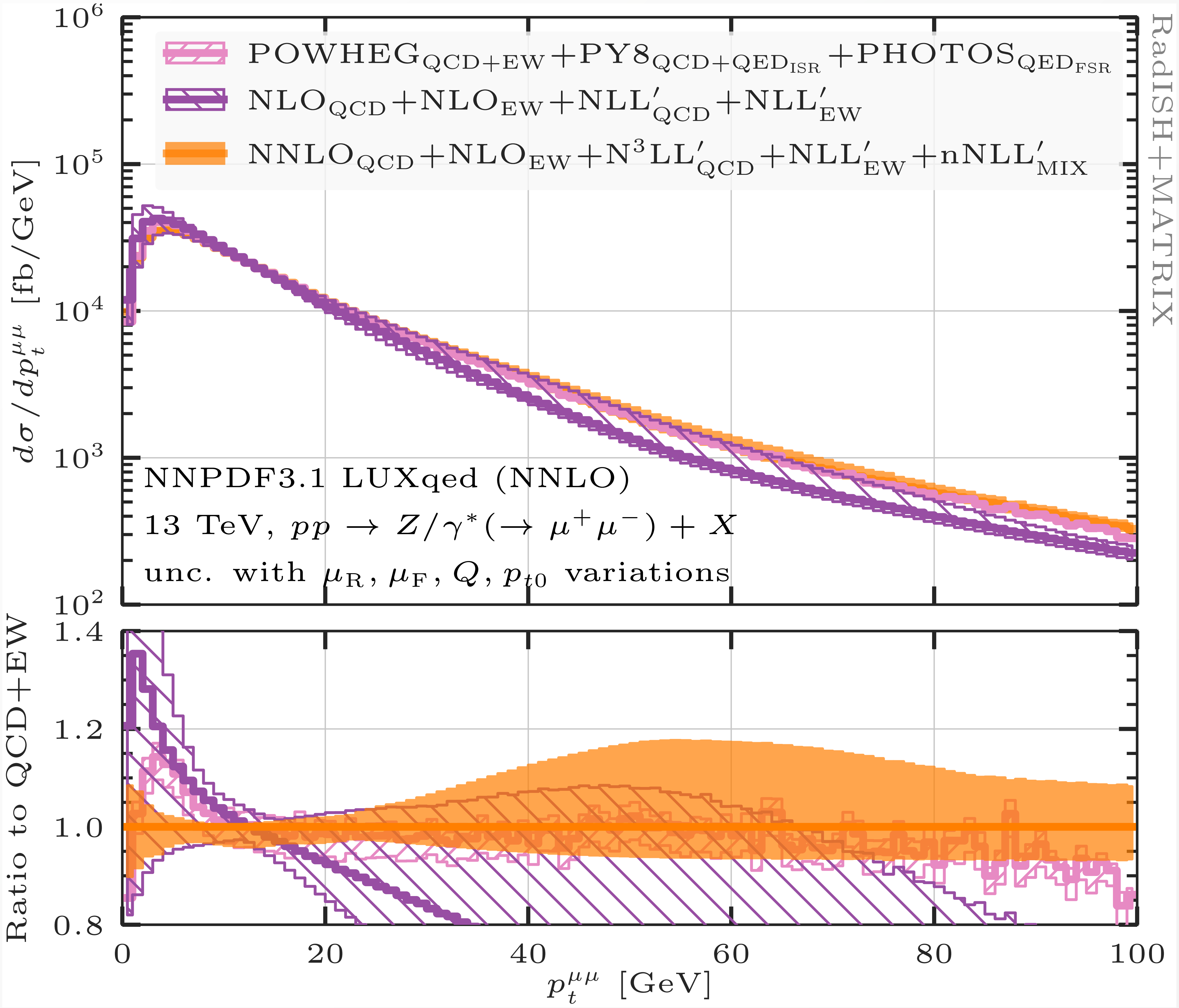

NLL$'_{EW}$+nNLL$'_{MIX}$ (including non-factorisable contributions) resummation **available for the first time at the level of bare muons**, allowing for a level of flexibility comparable to that of dedicated EW MC generators
[Buonocore, LR, Torrielli 2024]

Availability of such a tool allows to compare QED showers to predictions with higher formal accuracy

Alternative assessment of robustness of QED FSR treatment in current analyses

Conclusion

- Modelling of theoretical uncertainties crucial for EW precision programme at the LHC
- Resummation needed for observable sensitive to soft/collinear radiation. Different resummation approaches differ by subleading logarithmic and/or higher orders terms, whose relevance should be assessed
- Work in progress in the subgroup, with different theory groups providing their best predictions and benchmarking their results
- Perturbative QCD predictions have reached a remarkable level of accuracy. Comprehension of NP physics, PDF uncertainty (including MHOU), interplay with QED/mixed QCD/EW predictions mandatory for a successful precision programme
- Monte Carlo tunes for sub-percent precision must be handled with care. Availability of accurate perturbative calculation may provide insight on tuning parameters to avoid unphysical correlations

Backup

Logarithmic accuracy and counting

Ingredients needed to reach a given logarithmic accuracy

	Boundary conditions (FO hard, coll., soft)	Anomalous dimensions γ_i	$\Gamma_{\mathrm{cusp}}, \beta$	FO matching (nonsingular)
LL	1	-	1-loop	-
NLL	1	1-loop	2-loop	-
NLL′+NLO$_0$	α_s	1-loop	2-loop	α_s
NNLL+NLO$_0$	α_s	2-loop	3-loop	α_s
NNLL′+NNLO$_0$	α_s^2	2-loop	3-loop	α_s^2
N^{3}LL+NNLO$_0$	α_s^2	3-loop	4-loop	α_s^2

Credits: F. Tackmann

E.g. in *b* space, in a **very** schematic way

$$\Sigma_{\mathrm{NNLL}}(v) \sim \exp[Lg_0(\alpha_s L) + g_1(\alpha_s L) + \alpha_s g_2(\alpha_s L)]$$

$$\Sigma^{(1)}_{\mathrm{NNLL}}(v) \sim \exp[Lg_0(\alpha_s L) + g_1(\alpha_s L)](1 + \alpha_s g_2(\alpha_s L) + \dots)$$

$$\Sigma^{(2)}_{\mathrm{NNLL}}(v) \sim \exp[Lg_0(\alpha_s L) + g_1(\alpha_s L) + \alpha_s \tilde{g}_2(\alpha_s L)]\{1 + \alpha_s[g_2(\alpha_s L) - \tilde{g}_2(\alpha_s L)] + \dots\}, \qquad \tilde{g}_2(x) \neq g_2(x)$$

Results all **formally equivalent** at NNLL accuracy

Logarithmic accuracy and counting: the role of DGLAP evolution

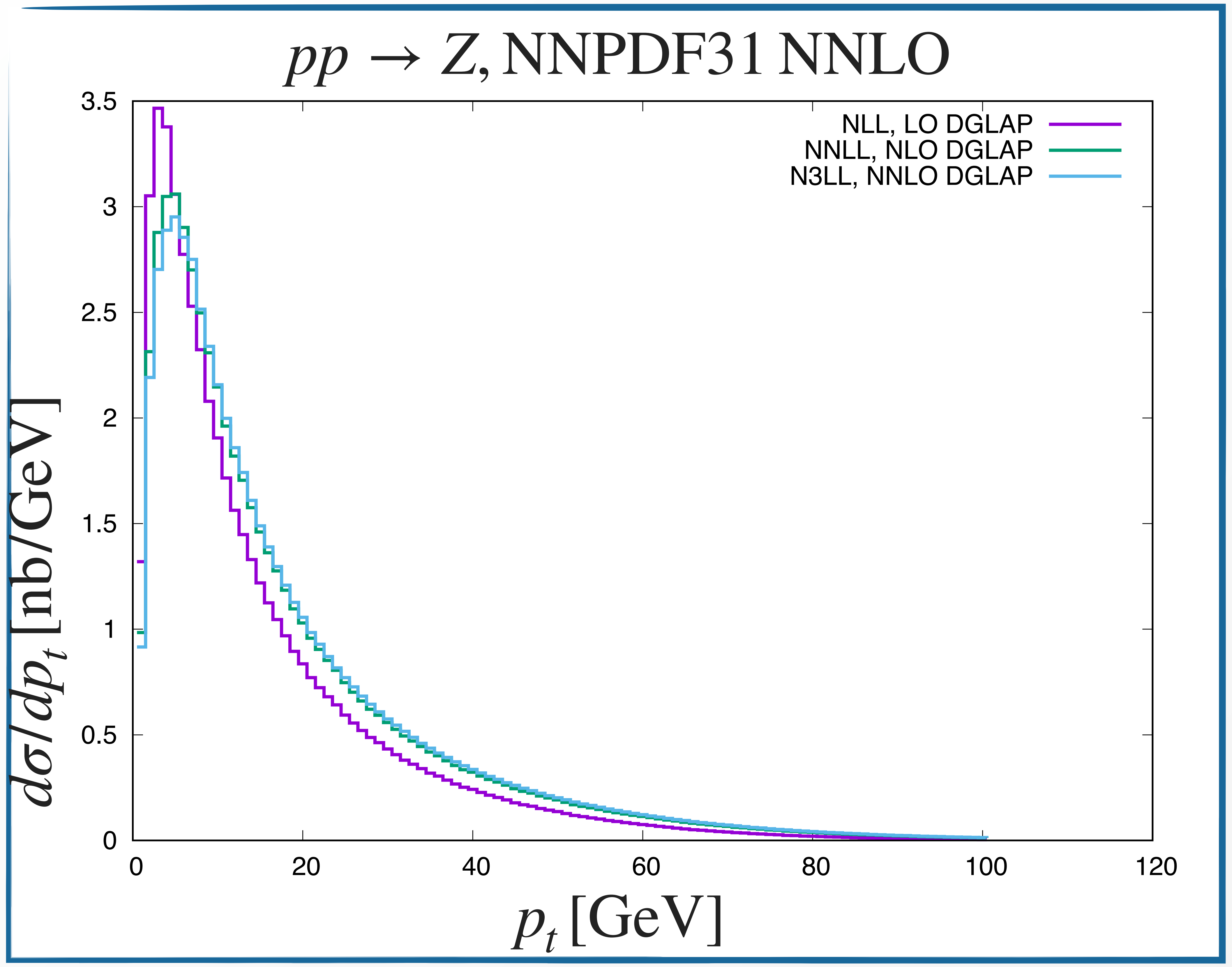

Ev. at LO, NLO, NNLO at NLL, NNLL, N^{3}LL

Default in e.g. DYRes/DYTURBO, ReSolve

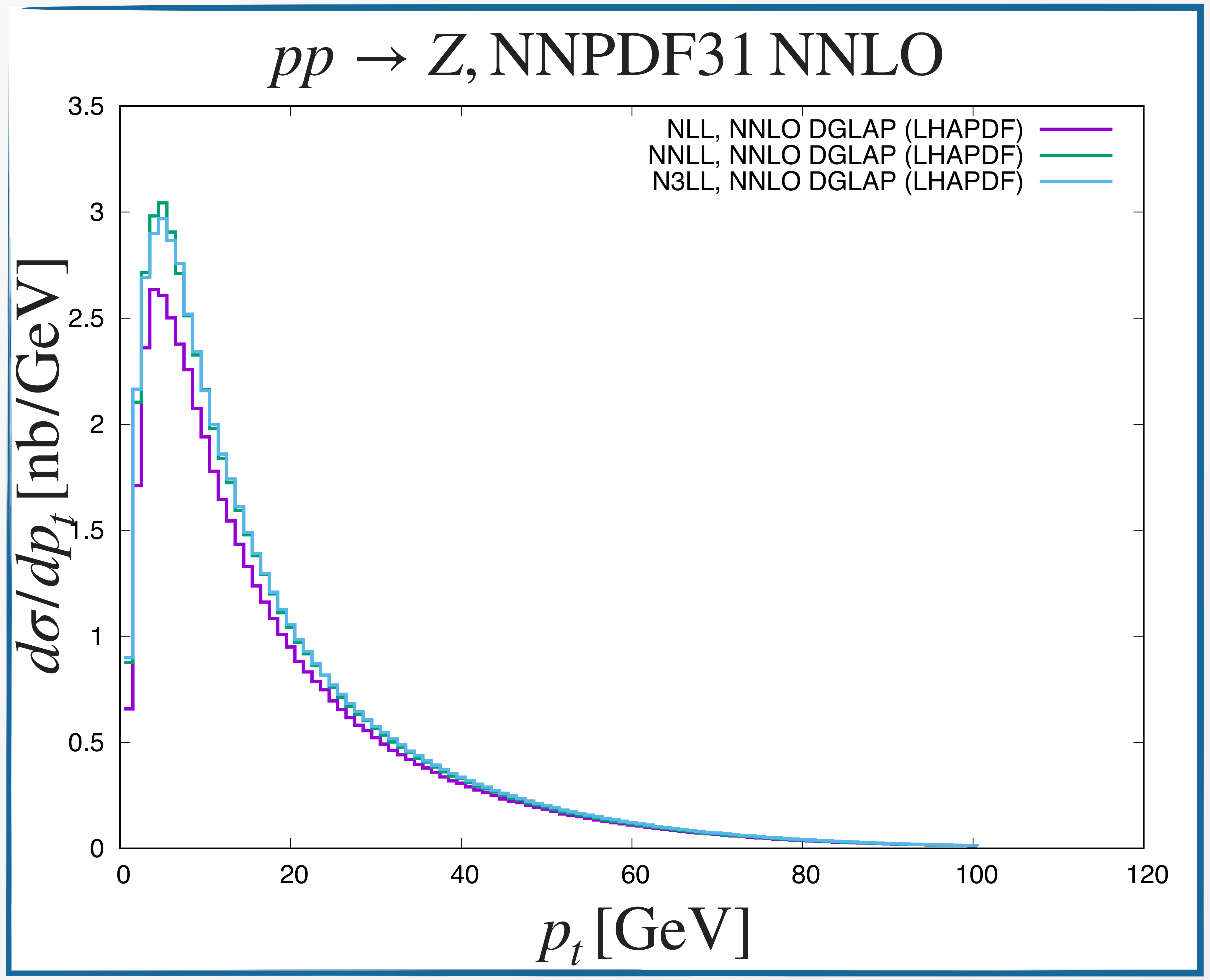

Ev. at NNLO at NLL, NNLL, N^{3}LL via LHAPDF

Default in e.g. RadISH, ResBos2, SCETLib

Advantage in using LHAPDF: (partial) information on quark thresholds

Differences **can be important** at NLL and NNLL and are an indication of the size of subleading corrections

b-space results vs. p_t space results

For codes whose formal accuracy is defined in b-space, it may be of some interest to compare the results both in impact-parameter space and in p_t-space after the inverse Fourier transform

Joshua Isaacson, ResBos2

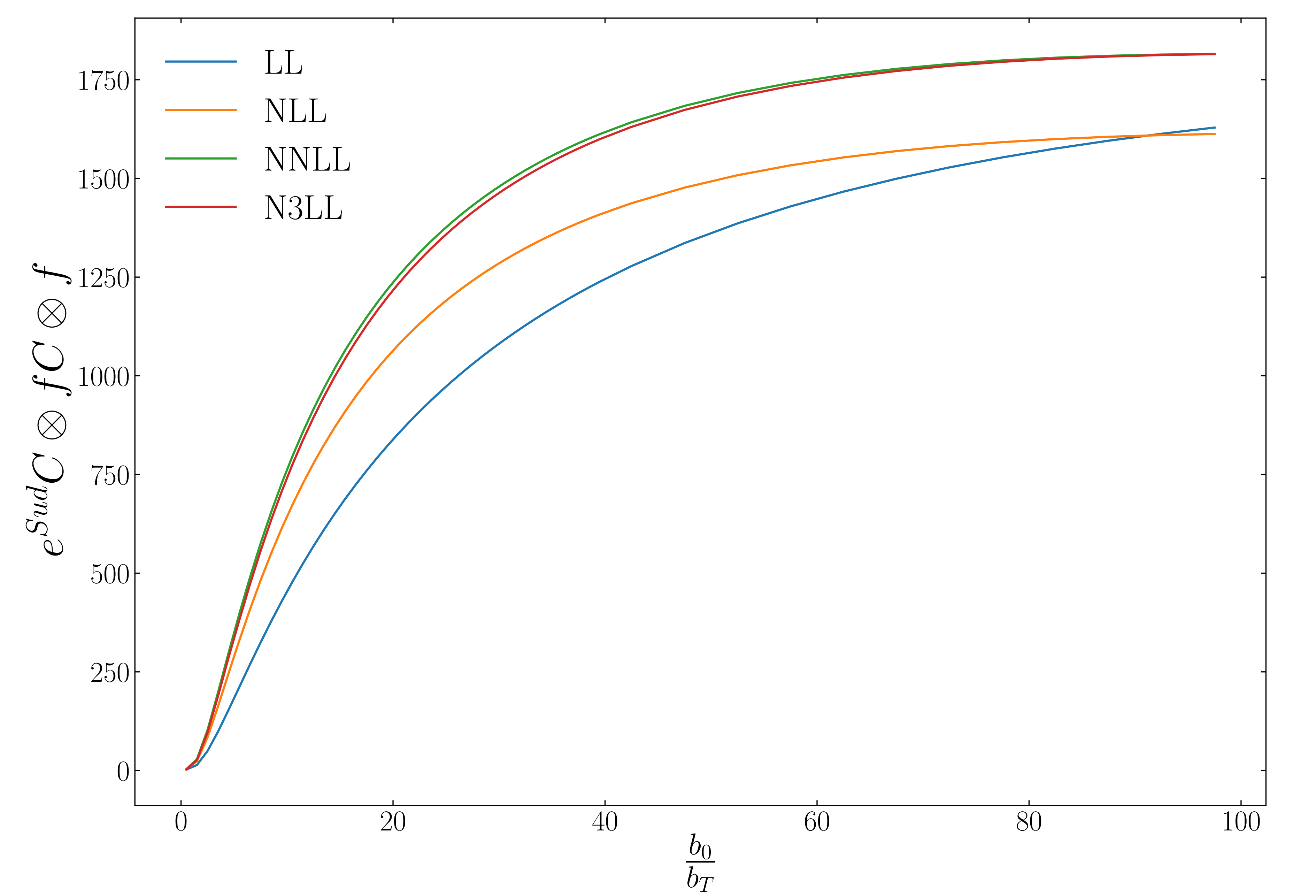

Inverse Fourier Transform

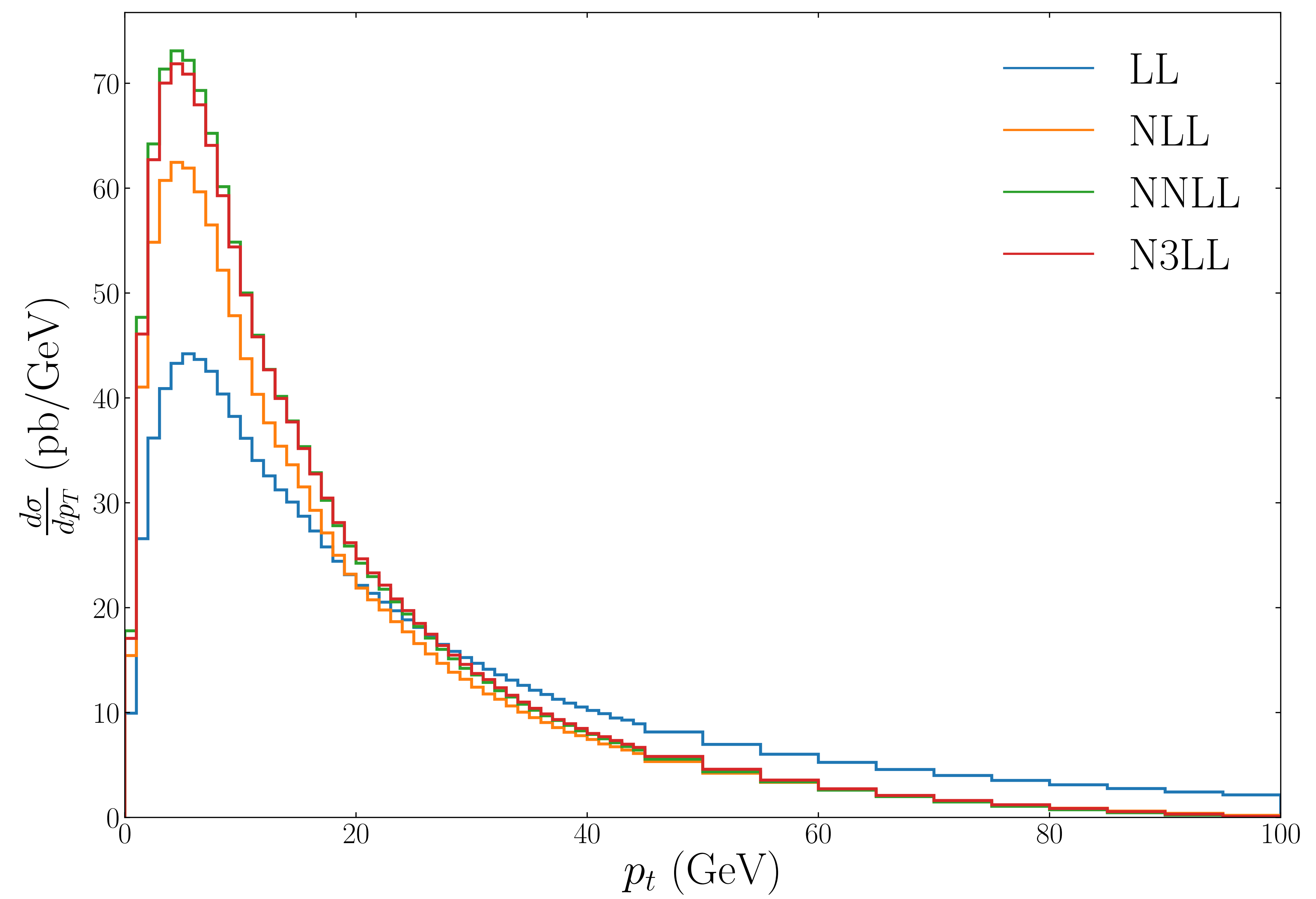

Matching ambiguities

F. Coradeschi/T. Cridge, ReSolve

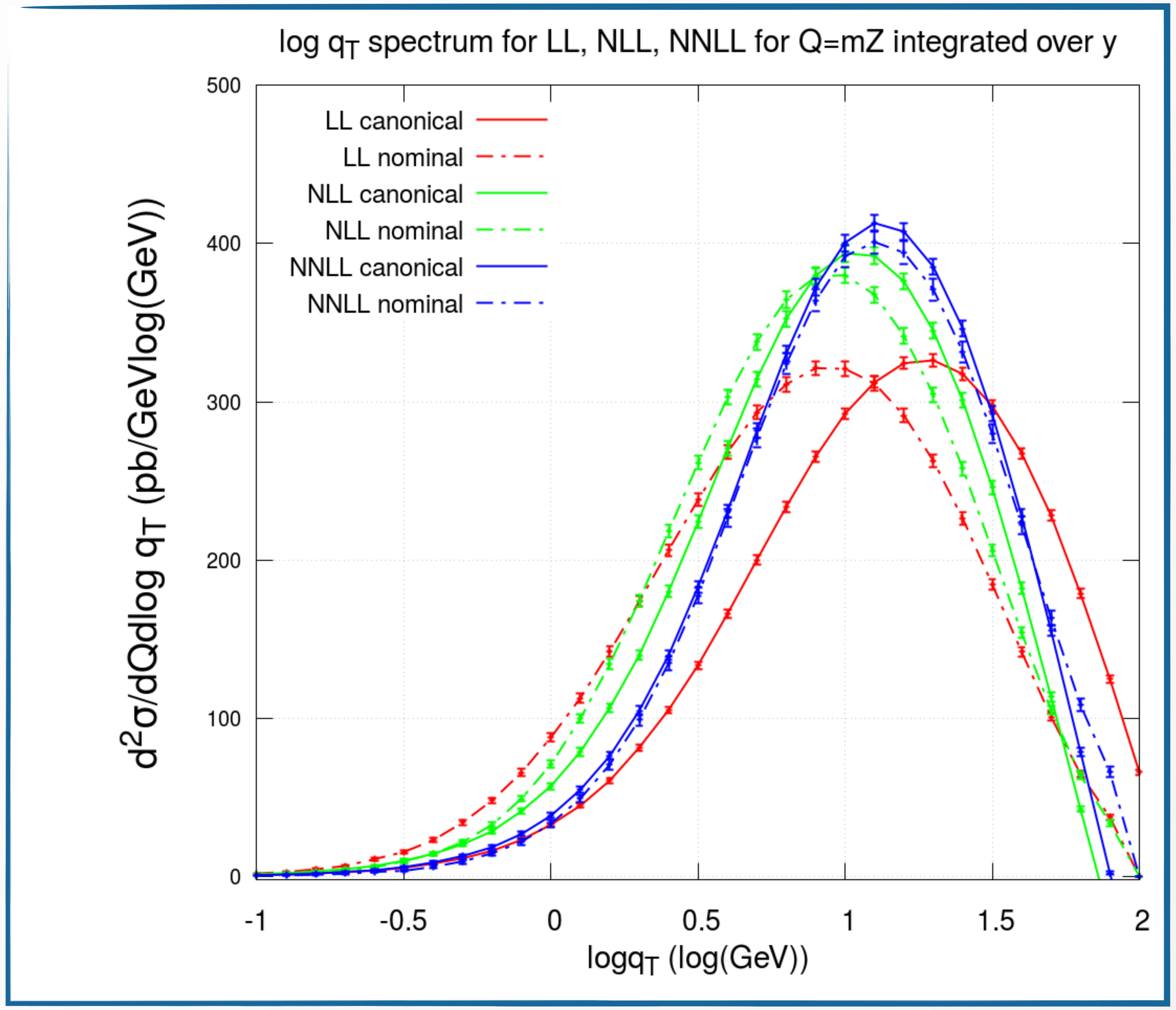

Nominal (**un-modified**) vs. canonical (**modified**) logs
most of the differences due to the different resummation scales used in the two cases

T. Becher, CuTe

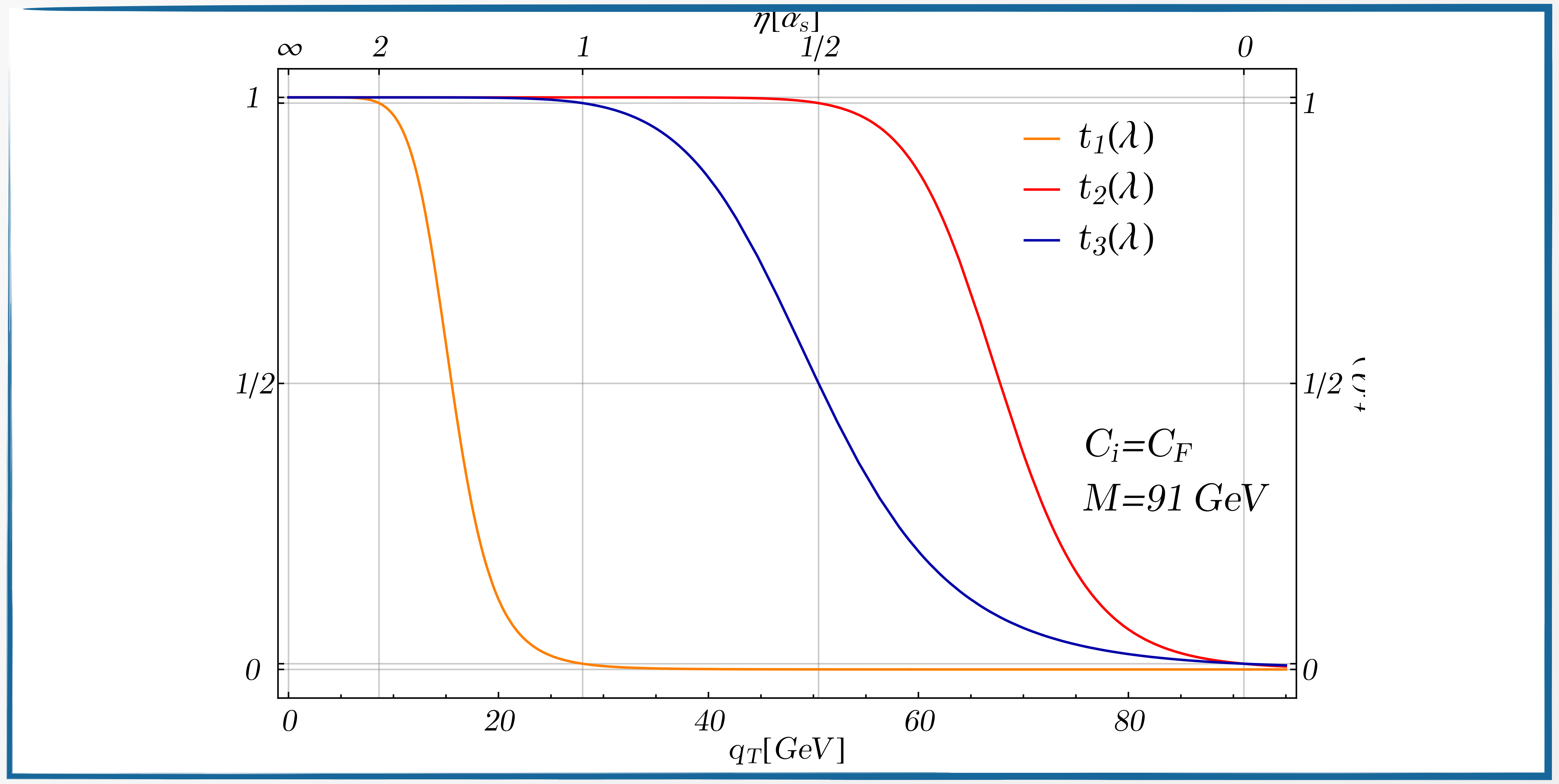

Transition functions and matching functions used to turn off resummation at large q_t

$$\frac{d\sigma_{\rm ms}}{dq_T} = t(\lambda)\frac{d\sigma_{\rm res}}{dq_T} + \left[R_{\rm sud}(\mu_{\rm ms})\right]^{t(\lambda)}\left[\frac{d\sigma_{\rm fo}}{dq_T} - t(\lambda)\frac{d\sigma_{\rm sqt}}{dq_T}\right]$$

Matching details play an important role in the transition region, but at lower accuracy might induce differences also in the small-p_t limit

Non-perturbative corrections

1. All formalisms have to deal with the **Landau pole**

- direct space: Sudakov radiator hit Landau pole at $\alpha_s(\mu_R^2)\beta_0 \ln Q/k_{t1} = \frac{1}{2}$

  n.b. since at small p_t the large azimuthal cancellations dominate, this cutoff is never an issue in practice

- b space, when integrating over b, the integral hits the Landau pole at large values of b
- Several solutions available

E.g. b* prescription: impact parameter frozen at a value $b_* = \frac{b}{\sqrt{1+(b/b_{\rm lim})}}, \quad b_* < b_{\rm lim}$

2. intrinsic quark transverse momentum (initial condition for TMDs)

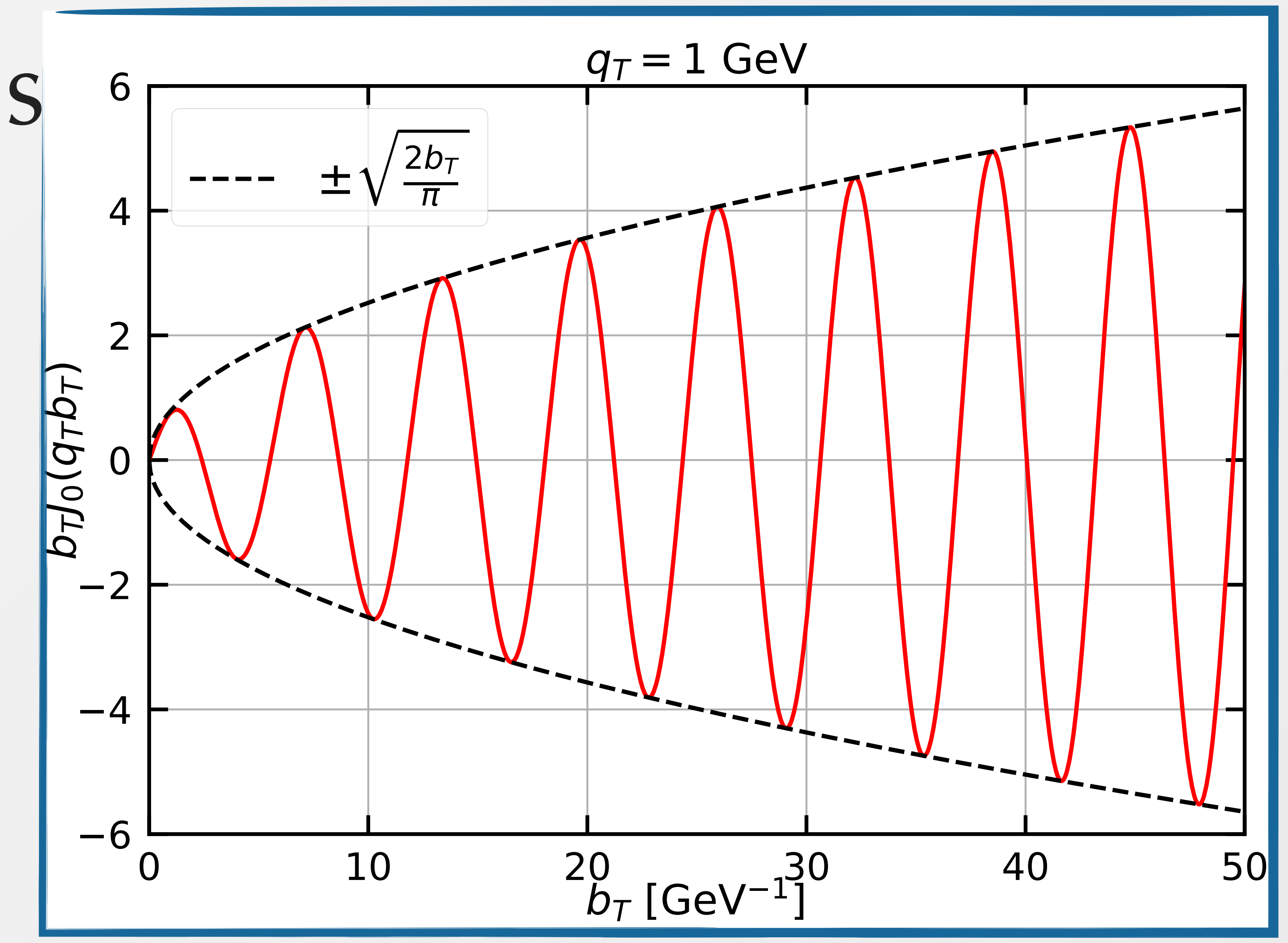

- **non-perturbative, fitted factor to model the non-perturbative region**, in principle kinematics- and flavour-dependent
- **Fitted factor** may help to stabilize the numerical integral when computing b-integral

V. Bertone/G. Bozzi, NangaParbat

Heavy-quark effects

Bottom quarks in the initial state yield ~4% of the total Z cross section (CKM suppressed for W)

Collinear logarithmic contributions encoded in DGLAP evolution in the 5FS; accounting for bottom mass can be important at scales p_t ~ m_b ~ peak region

Existing studies indicate very small corrections ~ 1%

[Bagnaschi, Maltoni, Vicini, Zaro '18]

Exact shape details remain an open question: fully consistent treatment in resummations useful for %-level precision

[Aivazis, Collins, Olness, Tung '93]
[Nadolsky, Kidonakis, Olness, Yuan '02]
[Berge, Nadolsky, Olness '05]
[Pietrulewicz, Samitz, Spiering, Tackmann '17][

Full calculation still unavailable, but partial results indicate a percent effect at p_t~m_b

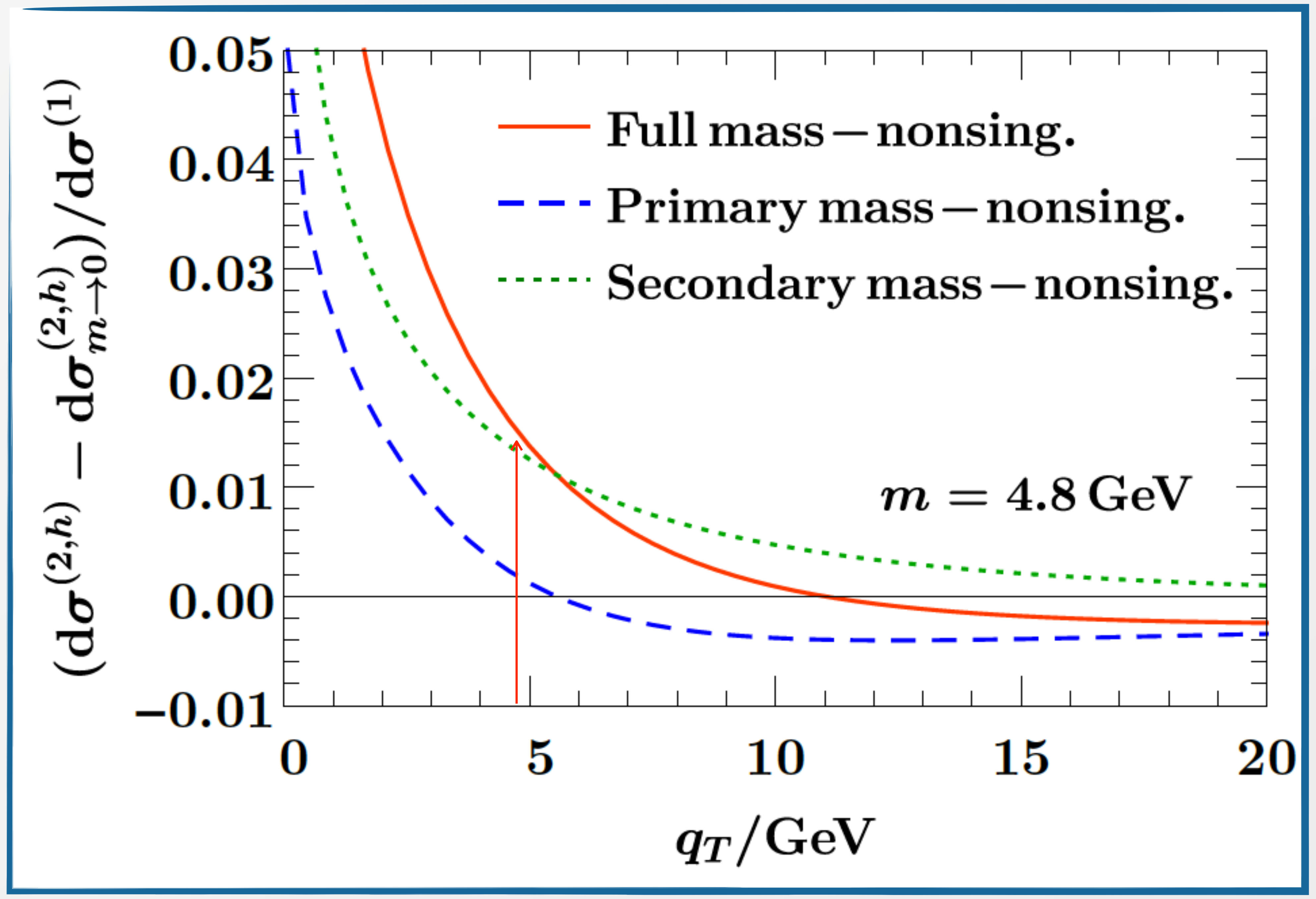

[Pietrulewicz, Samitz, Spiering, Tackmann '17]

EW corrections: ratio p_T^W / p_T^Z

Comparison with PWG$_{EW}$+PY8+PHOTOS, PWG$_{QCD}$+PY8+PHOTOS and $\mathrm{NLL}'_{\mathrm{QCD}} + \mathrm{NLO}_{\mathrm{QCD}} + \mathrm{NLL}'_{\mathrm{EW}} + \mathrm{NLO}_{\mathrm{EW}}$

- Nice perturbative stability and robustness against shower tuning
- Better agreement of "simpler" PWG$_{QCD}$+PY8+PHOTOS to RadISH, residual difference similar to pure QCD case
- PWG$_{EW}$+PY8+PHOTOS result deviates significantly from our best prediction